Deltares

Development of a 3D model for the NW European Shelf (3D DCSM-FM)

Development of a 3D model for the NW European Shelf (3D DCSM-FM)

Author(s)
Firmijn Zijl
Stendert Laan
Julien Groenenboom

Development of a 3D model for the NW European Shelf (3D DCSM-FM)

Client	Dutch Ministry of Infrastructure and Water Management
Contact	Martin Scholten Yann Friocourt
Reference	
Keywords	D-HYDRO, D-Flow Flexible Mesh, North Sea, NW European Continental Shelf, 3D DCSM-FM, hydrodynamic model

Document control	
Version	1.1
Date	15-02-2021
Project nr.	11205259-015
Document ID	11205259-015-ZKS-0003
Pages	61
Classification	
Status	final

Author(s)		

Doc. version	**Author**	**Reviewer**	**Approver**	**Publish**
1.0	Firmijn Zijl Stendert Laan Julien Groenenboom	Tony Minns	Toon Segeren	
1.1	Firmijn Zijl Stendert Laan Julien Groenenboom	Tony Minns	Toon Segeren	

Summary

In the past years, Deltares has worked on the development of a three-dimensional (3D) hydrodynamic model of the Northwest European Shelf: the 3D Dutch Continental Shelf Model in Flexible Mesh (3D DCSM-FM). Specifically, this model covers the North Sea and adjacent shallow seas and estuaries in the Netherlands, such as the Wadden Sea, the Ems-Dollard estuary, the Western Scheldt and the Eastern Scheldt. Rijkswaterstaat (Dutch Ministry of Infrastructure and Water Management) has requested Deltares to further develop and release this model as a sixth-generation model. As such, this development links to a more comprehensive project in which sixth-generation models are developed for all waters maintained by Rijkswaterstaat. An important difference with the previous fifth-generation models is the use of the Delft3D FM Suite (or D-HYDRO Suite), the new software framework for modelling free surface flows, which was first released in 2015 and allows for the use of unstructured grids.

While the previous fifth-generation models for the same area were specifically aimed at an optimal representation of water levels for operational forecasting under daily and storm surge conditions, for the sixth-generation models the scope is wider. This model should, for example, also be suitable to use for water quality and ecology studies, oil spill modelling, search and rescue. It must also provide three-dimensional (3D) boundary conditions (including temperature and salinity) for detailed models, which include the Haringvliet and Rhine-Meuse Delta (RMM). Also, the idea is to merge the separate model lines that existed for 2D and 3D models by reusing the 2D schematisation and barotropic forcing as much as possible in the 3D version of the model. Therefore, 3D DCSM-FM is based on the two-dimensional model DCSM-FM 0.5nm, which has been developed for the Dutch Ministry of Infrastructure and Water Management (Zijl and Groenenboom, 2019).

The main purpose of 3D DCSM-FM is to have a versatile model that can be used for all manner of studies and research on the Northwest European Continental Shelf, including the North Sea and adjacent shallow seas, such as the Wadden Sea. It aims to combine state-of-the-art capabilities with respect to modelling of water levels (tide and surge) as well as (residual) transport phenomena. The latter is crucial for application in water quality and ecological modelling.

Since the demands posed by the various applications are impossible to meet with one model, two horizontal schematizations (resulting in 3 models) are proposed and developed:

1. DCSM-FM 0.5nm: a relatively coarse schematization (minimum grid size of 800-900 m in Dutch waters). The corresponding computational time makes it possible to use for the following models:
   a. a 3D transport model, including temperature and salinity as state variables (3D DCSM-FM).
   b. 2D tide-surge model that is fast enough to produce probability forecasts with a 2 – 10 day lead-time. These forecasts will be based on meteorology of the ECMWF Ensemble Prediction System (EPS) and will replace the fourth-generation model DCSMv5 that is currently used for this application. The development of this model is described in Zijl & Groenenboom (2019).

2. DCSM-FM 100m: a relatively fine, 2D schematization with a minimum resolution of ~100 m in some Dutch waters (such as the Wadden Sea) to be used for accurate

(operational) water level forecasting. This model is based on the schematization in item 1, but with refinement where required. The development of this model is described in Zijl et al. (2020).

The present report deals with the development (model setup and validation) of the three-dimensional model 3D DCSM-FM. For reference purposes, this version of the model will also be referred to as dflowfm3d-noordzee_0_5nm-j17_6-v1.

With respect to validation and comparison against existing models, it was concluded that the quality of the representation of the tide is, averaged over all Dutch coastal stations, very similar to the two-dimensional sixth-generation model DCSM-FM 0.5nm, while the surge quality has improved by around 10%. This leads to a slightly better representation of total water levels. Comparison against the previous generation 3D ZUNO-DD model of the southern North Sea shows that the total water levels along the Dutch coast have improved by almost 75%, due to substantial improvements in both tide and surge. Furthermore, the model was validated against measured surface temperature and surface salinity, as well as measurements of seasonal temperature stratification in the central North Sea. The residual transport through the English Channel is also confirmed to be in the realistic range. Finally, recommendations are made for further development.

Contents

1 Introduction

1.1 Background

In the past years, Deltares has worked on the development of a three-dimensional (3D) hydrodynamic model of the Northwest European Shelf: 3D Dutch Continental Shelf Model in Flexible Mesh (3D DCSM-FM). Specifically, this model should cover the North Sea and adjacent shallow seas and estuaries in the Netherlands, such as the Wadden Sea, the Ems-Dollard estuary, the Western Scheldt and the Eastern Scheldt. Rijkswaterstaat (Dutch Ministry of Infrastructure and Water Management) has requested Deltares to further develop and release this model as a sixth-generation model. As such, this development links to a more comprehensive project in which sixth-generation models are developed for all waters maintained by Rijkswaterstaat. An important difference with the previous fifth-generation models is the use of the Delft3D FM Suite (or D-HYDRO Suite[1]), the new software framework for modelling free surface flows, which was first released in 2015 and allows for the use of unstructured grids. Eventually, all fifth-generation models will be replaced with a sixth-generation equivalent.

The existing fifth-generation models for the NW European Shelf and North Sea (DCSMv6 and DCSMv6-ZUNOv4, see Zijl (2013)) were depth-averaged models, specifically aiming at an optimal representation of water levels for operational forecasting under daily and storm surge conditions. Furthermore, there is an existing 3D model of the southern North Sea, ZUNO-DD, which is commonly used as a basis for water quality and ecology studies. For the sixth-generation models the scope is wider; the model should, for example, also be suitable to use for water quality and ecology studies, oil spill modelling, search and rescue. It must also provide three-dimensional (3D) boundary conditions (including temperature and salinity) for detailed models. which include the Haringvliet and Rhine-Meuse Delta (RMM). Also, the idea is to merge the separate model lines that existed for 2D and 3D models by reusing the 2D schematisation and barotropic forcing as much as possible in the 3D version of the model. Therefore, 3D DCSM-FM is based on the two-dimensional model DCSM-FM 0.5nm, which has been developed for the Dutch Ministry of Infrastructure and Water Management (Zijl and Groenenboom, 2019).

The main purpose of 3D DCSM-FM is to have a versatile model that can be used for all manner of studies and research on the Northwest European Continental Shelf, including the North Sea and adjacent shallow seas, such as the Wadden Sea. It aims to combine state-of-the-art capabilities with respect to modelling of water levels (tide and surge) as well as (residual) transport phenomena. The latter is crucial for application in water quality and ecological modelling. By combining this, the model is ideally suited for this study.

The above applications pose a wide range and sometimes mutually exclusive demands on a model. This is because both the relative importance of representing certain phenomena as well as the allowed computational time varies per application. Since the demands are impossible to meet with one model, two horizontal schematizations (resulting in 3 models) were proposed and developed:

[1] D-HYDRO Suite is the Dutch name of Delft3D-FM Suite. The two names, D-HYDRO and Delft3D-FM are therefore interchangeable throughout this report.

1. DCSM-FM 0.5nm: a relatively coarse schematization (minimum grid size of 800-900 m in Dutch waters). The corresponding computational time makes it possible to use for the following models:
    a. a 3D transport model, including temperature and salinity as state variables (3D DCSM-FM).
    b. 2D tide-surge model that is fast enough used to produce probability forecasts with a 2 – 10 day lead-time. These forecasts will be based on meteorology of the ECMWF Ensemble Prediction System (EPS) and will replace the fourth-generation model DCSMv5 that is currently used for this application. The development of this model is described in Zijl & Groenenboom (2019).
2. DCSM-FM 100m: a relatively fine 2D schematization with a minimum resolution of ~100 m in some Dutch waters (such as the Wadden Sea) to be used for accurate (operational) water level forecasting. This model is based on the schematization in item 1, but with refinement where required. The development of this model is described in Zijl et al. (2020).

The present report deals with the development of the three-dimensional model 3D DCSM-FM. For reference purposes, this version of the model will also be referred to as dflowfm3d-noordzee_0_5nm-j17_6-v1.

To ensure that all sixth-generation models are compatible, the guidelines with generic technical and functional specifications as specified in (Minns et al., 2019) were used during the setup of this model.

1.2 Guide to this report

The next chapters describe the setup of 3D DCSM-FM (Chapter 2). In Chapter 3 the water level validation is presented. The focus in Chapter 4 is on the validation of salinity, temperature and residual currents in the model. The report ends with conclusions and recommendations in Chapter 5.

2 Model setup

2.1 Introduction

The 3D hydrodynamic model of the Northwest European Shelf (3D DCSM-FM) builds on the depth-averaged DCSM-FM 0.5nm model, which has been developed for RWS. Therefore, the horizontal schematization and the lateral barotropic forcing of both models are mostly the same. Where changes are made in settings and model forcing, these are explicitly mentioned in this report. In contrast to the 2D model, transport of salinity and temperature has also been added to this model. This necessitates additional lateral boundary and surface boundary forcing, as well as the inclusion of fresh-water river discharges throughout the domain.
The model development, calibration and validation of the depth-averaged DCSM-FM 0.5nm is reported in Zijl & Groenenboom (2019). To make this report easier to read, all model aspects are at least briefly repeated here, even though some are unchanged compared to the 2D version of the model. In addition, an overview of differences between both models is presented in section 2.10.

2.2 Network

2.2.1 Network coverage, horizontal extent

3D DCSM-FM covers the Northwest European Continental Shelf, specifically the area between 15°W to 13°E and 43°N to 64°N (see Figure 2.1). This means that the open boundary locations are the same as in the fifth-generation model DCSMv6 (Zijl et al., 2013).

2.2.2 Grid size

One of the advantages of Delft3D Flexible Mesh is the enhanced possibility to better match resolution with relevant local spatial scales. Compared to a structured grid approach, the new flexible mesh has coarser grid cells near the open boundaries and in deep waters, whereas the resolution increases toward the shallower waters. The advantage of coarsening in deep areas in particular is twofold: Firstly, it reduces the number of cells in areas where local spatial scales allow it; and secondly it eases the numerical time step restriction. On the other hand, in shallow areas, resolution plays an important role in accurately representing tide and surge, including its enhanced non-linear interaction.

Given the above considerations, the DCSM-FM network was designed to have a resolution that increases with decreasing water depth. The starting point was a network with a uniform cell size of 1/10° in east-west direction and 1/15° in north-south direction. This coarse network was refined in three steps with a factor of 2 by 2. The areas of refinement were specified with smooth polygons that were approximately aligned with the 800 m, 200 m and 50 m isobaths (i.e., lines with equal depth). Areas with different resolution are connected with triangles. The choice of isobaths ensures that the cell size scales with the square root of the depth, resulting in relatively limited variations of wave Courant number within the model domain.

Other considerations in positioning the refinements were the number of cells between transitions (at least a few). Also, it was ensured that all coastlines, except very small islands, were covered by a few rows of the highest resolution cells. This implies that in areas with steep coasts the transition to the highest resolution takes place in deeper water. Another exception was made for the southern North Sea, where the area of highest resolution was expanded. This was done to ensure that the highly variable features in the bathymetry can properly be represented on the network. Furthermore, it ensures that the areas where steep salinity gradients can be expected are within the area with the highest resolution.

The resulting network is shown in Figure 2.2 and has approximately 630,000 cells with a variable resolution. The largest cells (shown in yellow) have a size of 1/10° in east-west direction and 1/15° in north-south direction, which corresponds to about 4 x 4 nautical miles (nm) or 4.9-8.1 km by 7.4 km, depending on the latitude. Along all coasts and in the southern North Sea, cell sizes decrease to 3/4’ in east-west direction and 1/2’ in north-south direction (shown in red). This corresponds to about 0.5 nm x 0.5 nm, which corresponds to approximately 900 m.

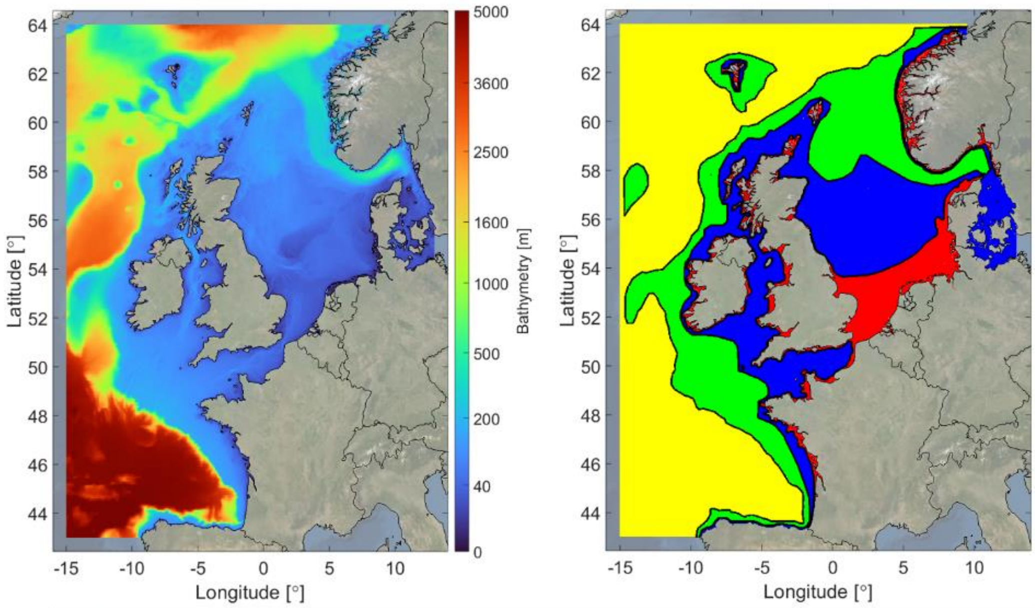

Yellow:	1/10° x 1/15°	~ 4.0 nm x 4.0 nm	
Green:	1/20° x 1/30°	~ 2.0 nm x 2.0 nm	→800m isobath
Blue:	1/40° x 1/60°	~ 1.0 nm x 1.0 nm	→200m isobath
Red:	0.75’ x 0.5’	~ 0.5 nm x 0.5 nm	→ 50m isobath

Figure 2.1 Bathymetry and grid cell sizes in 3D DCSM-FM

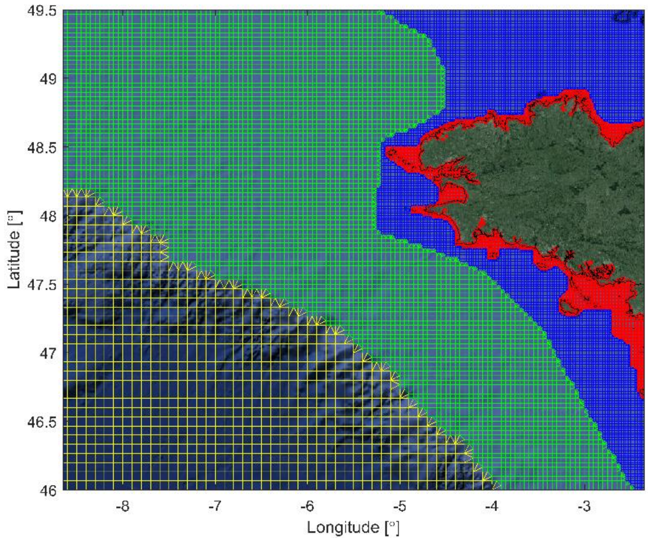

Figure 2.2 Computational grid shown in detail: quadrilateral cells with triangular cells at the transitions in resolution

2.2.3 Network optimization

The computational time step used is automatically limited by D-Flow FM (hydrodynamic module of D-HYDRO) based on a Courant criterium. This means that parts of the network with a combination of small flow links and high velocities are most likely to restrict the time step and consequently increase the computational time. To allow for a larger time step and consequently a faster computation, the grid was improved at the locations of the restricting cells. More information on the iterative procedure of optimizing the network see Zijl & Groenenboom (2019).

2.2.4 Vertical grid

A sigma-layer approach is used for the vertical schematization of the model. This implies that a fixed number of layers, with a thickness dependent on local water depth, is present. This results in a high vertical resolution in shallow areas. A total of 20 layers with a uniform thickness of 5% of the water column is applied.

2.3 Land-sea boundary, dry points and thin dams

After the local refinement of the network, the cells that covered land were removed from the computational domain. The first step was to interpolate the EMODnet bathymetric data to the grid and to delete all cells that do not have EMODnet data in its vicinity. Subsequently, a land-sea boundary obtained from the World Vector Shoreline (https://shoreline.noaa.gov/) was used to distinguish between land and water. All cells that, according to this land-sea boundary, were covered by more than 40% land were made inactive by specifying so-called dry points. The creation of these dry points was done automatically by a MATLAB-script. Figure 2.3 shows an overview of the resulting computational domain in the southwestern part of the Netherlands. The black line indicates the land-sea boundary and the red crosses within the grid illustrate the dry points.

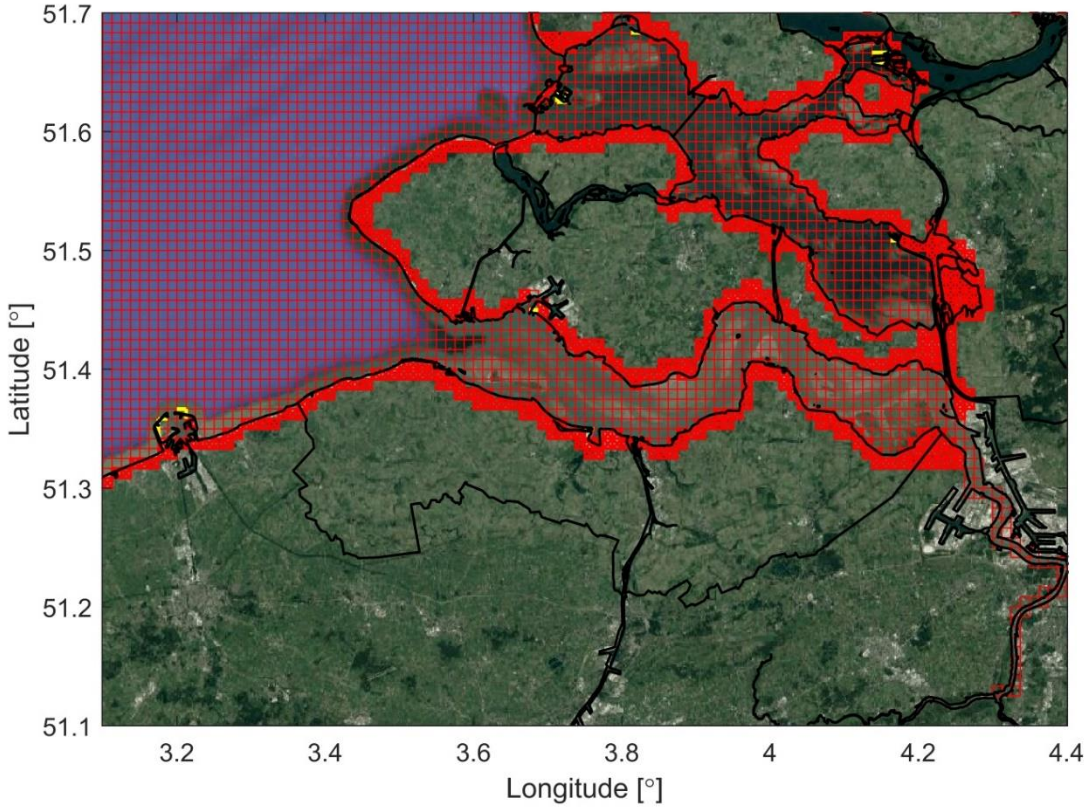

Figure 2.3 Overview of the computational grid (red), land-sea boundary (black), dry points (red crosses) and thin dams (yellow) in the Southwest Delta.

After this automated creation of a first set of dry points, manual work was necessary to get to the final version of the model geometry. During visual inspection of the shorelines, dry cells were added or removed where necessary. In addition, features that are relatively small compared to the area of a cell, are captured in the model schematisation by specifying so-called *thin dams*. These thin dams prohibit flow exchange through cell edges. The thick, yellow lines in Figure 2.4 illustrate how the entrance to the Humber Estuary (in which tide gauge station Immingham is located) and the breakwaters of the port of IJmuiden are represented by thin dams.

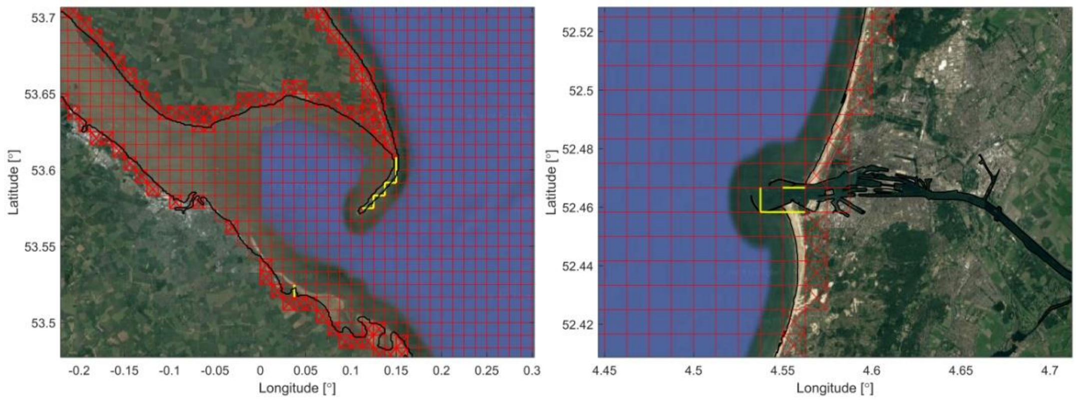

Figure 2.4 Overview of the computational grid (red), land-sea boundary (black), dry points (red crosses) and thin dams (yellow) in the Humber Estuary (left) and around the harbour of IJmuiden (right).

Another example of manual adjustments is at a couple of fjords in Norway. Some fjords consist of very small inlets that are connected to relatively large upstream basins. In some inlets, a dry point was added since the threshold of 40% land was exceeded and this resulted in blockage of flow to these upstream basins. Also, these erroneously created dry points were removed from the model schematisation. The resulting geometry near one of the many fjords in Norway is shown in Figure 2.5.

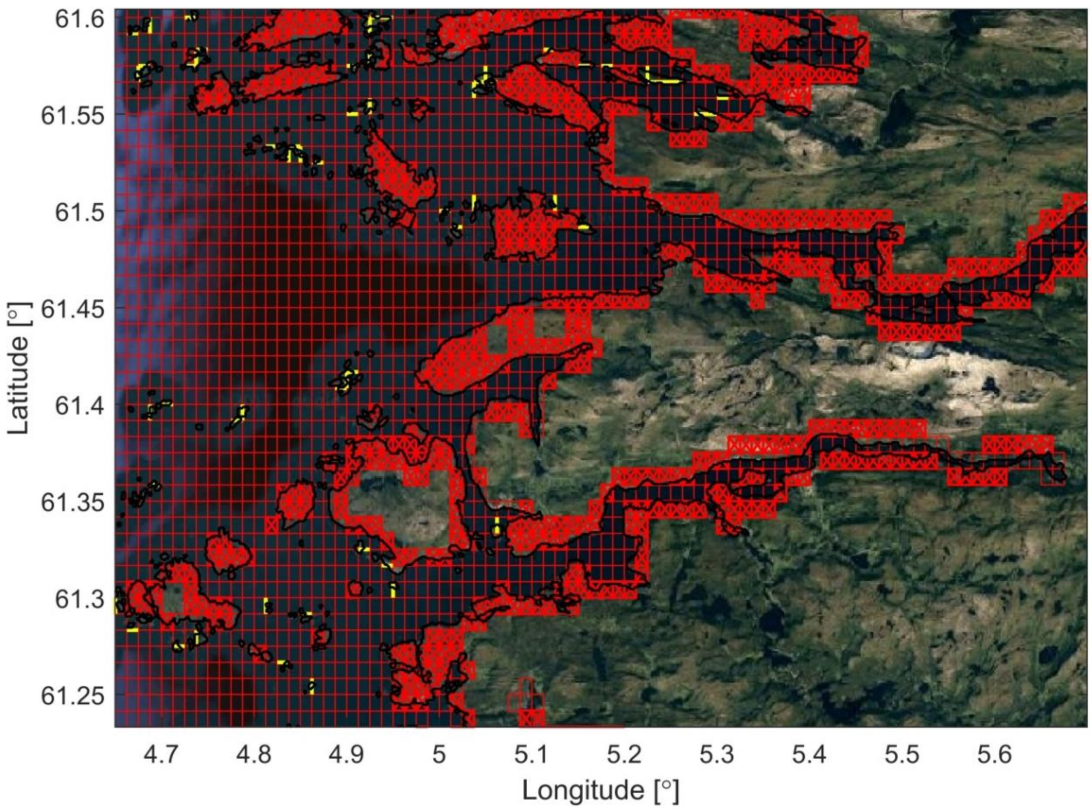

Figure 2.5 Overview of the computational grid (red), land-sea boundary (black), dry points (red crosses) and thin dams (yellow) in Norway.

In order to simulate the correct effect of estuaries on the hydrodynamics, not only certain automatically created dry points had to be removed but also additional grid cells were added to the model domain. Since the removal of grid cells was based on the availability of EMODnet data in the vicinity of the grid cell, some estuaries were not included in the model domain as no bathymetry data was available at these locations. Based on the land-sea boundary and Google Earth, the computational grid at the largest and most important estuaries that were not automatically incorporated in the model domain were manually added.

2.4 Bathymetry

The DCSM-FM model bathymetry has been derived from a gridded bathymetric dataset (October 2016 version) from the European Marine Observation and Data Network (EMODnet; EMODnet Bathymetry Consortium, 2016), a consortium of organisations assembling European marine data, metadata and data products from diverse sources. The data are compounded from selected bathymetric survey data sets (single and multi-beam surveys) and composite DTMs, while gaps with no data coverage are completed by integrating the GEBCO 30'' gridded bathymetry. The resolution of the gridded EMODnet dataset is 1/8' x 1/8' (approx. 160 x 230 m).

The EMODnet bathymetry data (October 2016 version) is only provided relative to Lowest Astronomical Tide (LAT). To make these data applicable for DCSM-FM, the bathymetric data was converted to the Mean Sea Level (MSL) vertical reference plane. The LAT-MSL relation was derived from a 19-year tide-only simulation (calendar years 2005 to 2023) with the previous generation DCSMv6. The long duration is required to capture an entire 18.6-year nodal cycle. For more information about the applied LAT-MSL relation, it is referred to the 2D DCSM-FM 0.5nm report (Zijl & Groenenboom, 2019).

For large parts of the Dutch waters, bathymetric information from the detailed Baseline database by the Dutch government is used.

The model bathymetry is provided on the net nodes. Depths at the middle of the cell edges (the velocity points) are set to be determined as the mean value of the depth at the adjacent nodes. Depths at the location of the cell face (the water level points) are specified to be determined as the minimum of the depth in the surrounding cell edges. These bathymetry interpolations options are prescribed by setting *bedlevtype=3*.

An overview of the resulting model bathymetry is presented in Figure 2.6. This shows that depths of more than 2000 m occur in the northern parts of the model domain, with depths exceeding 5000 m in the south-western part. The North Sea is much shallower with depths rarely exceeding 100m in the central and southern part (Figure 2.7). In Figure 2.8 a detail of the DCSM-FM model bathymetry is shown focussing on the southern North Sea. In the southern North Sea depths are generally less than 50 m.

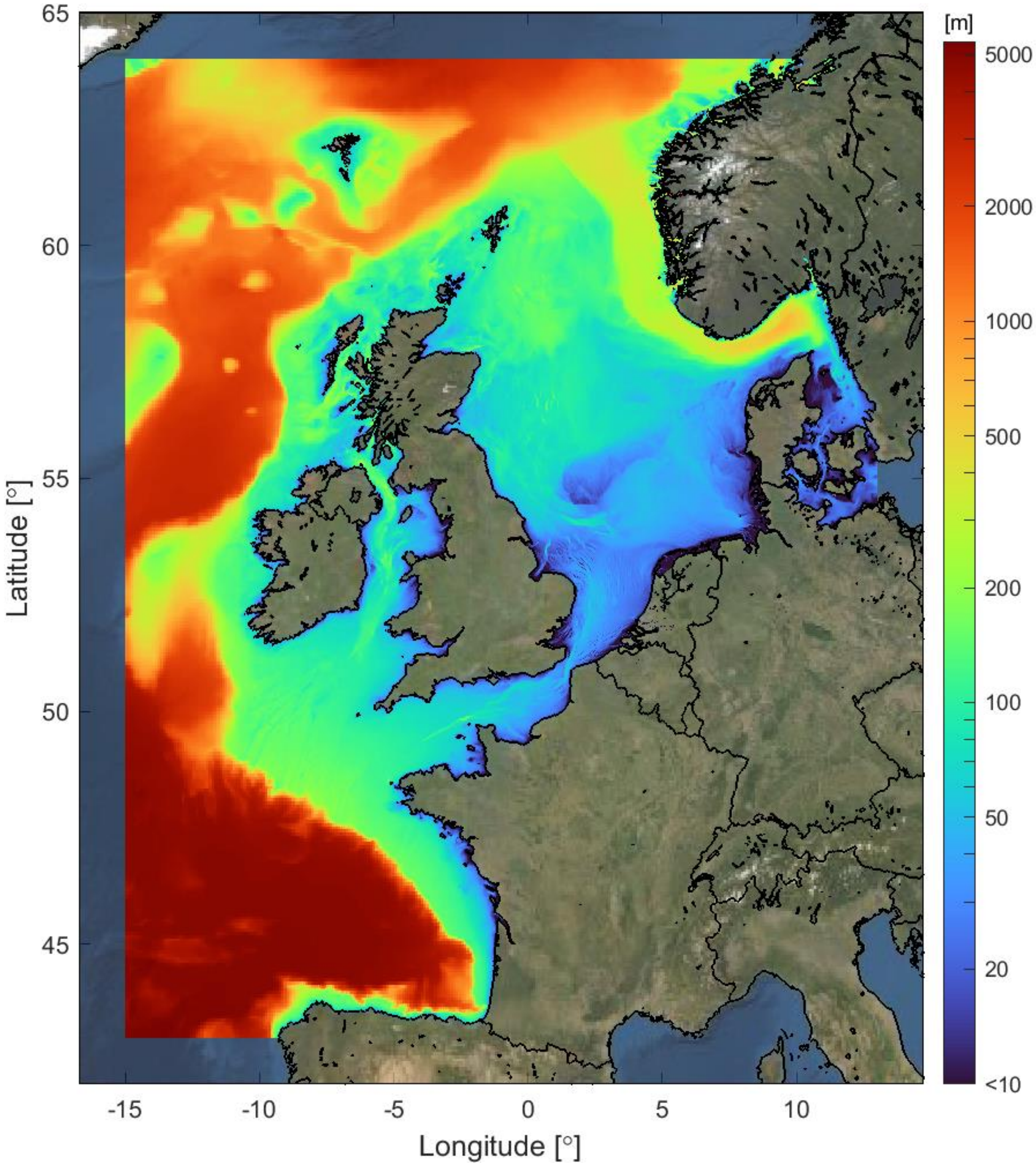

Figure 2.6   Overview of the DCSM-FM model bathymetry on a logarithmic scale (depths relative to MSL).

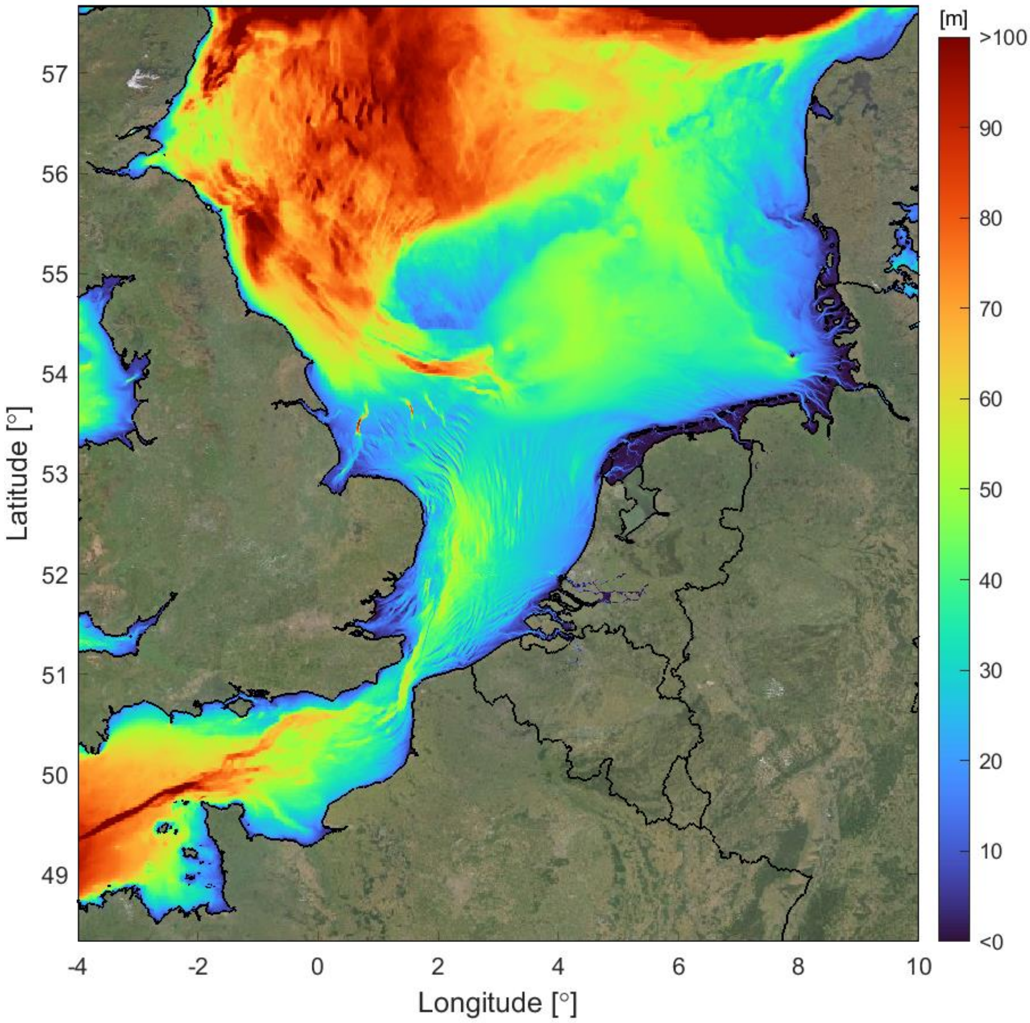

Figure 2.7 DCSM-FM model bathymetry in the central and southern North Sea (depths relative to MSL).

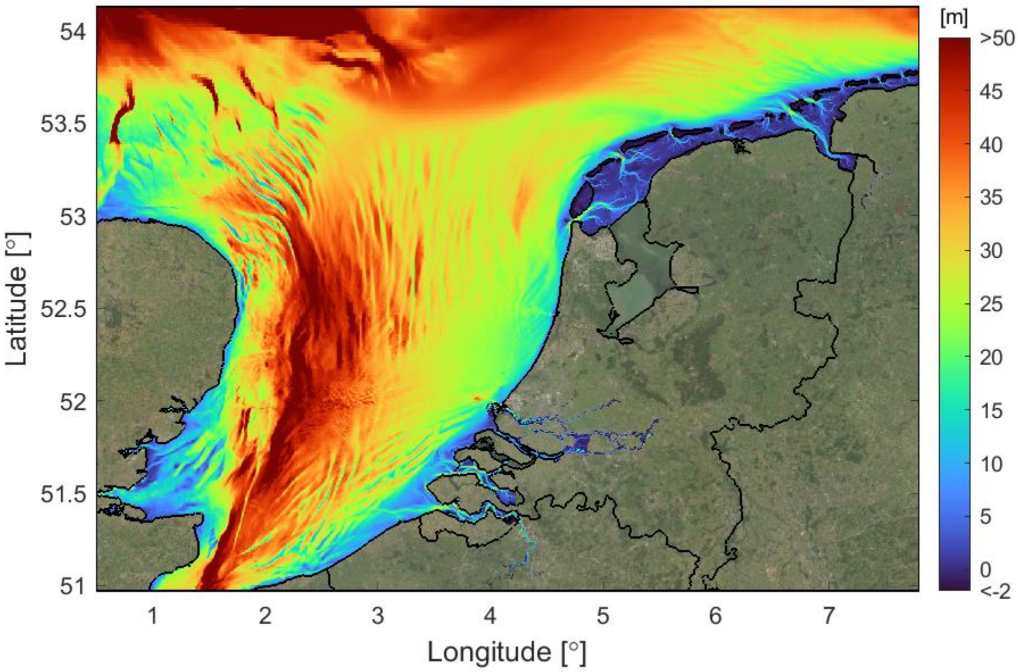

Figure 2.8 DCSM-FM model bathymetry in the southern North Sea (depths relative to MSL).

2.5 Bottom roughness

For the bed friction, a spatially varying Manning roughness coefficient is used. During the model calibration, using OpenDA-DUD, these values were adjusted to obtain an optimal water level representation. For the calibration of the bed roughness the model was run in 2D mode for the entire year of 2017, using more than 200 tide gauge stations shelf-wide (Zijl & Groenenboom, 2019).

The resulting roughness fields are presented in Figure 2.9 and Figure 2.10. The minimum and maximum bottom roughness values applied are 0.012 s/m$^{1/3}$ and 0.050 s/m$^{1/3}$.

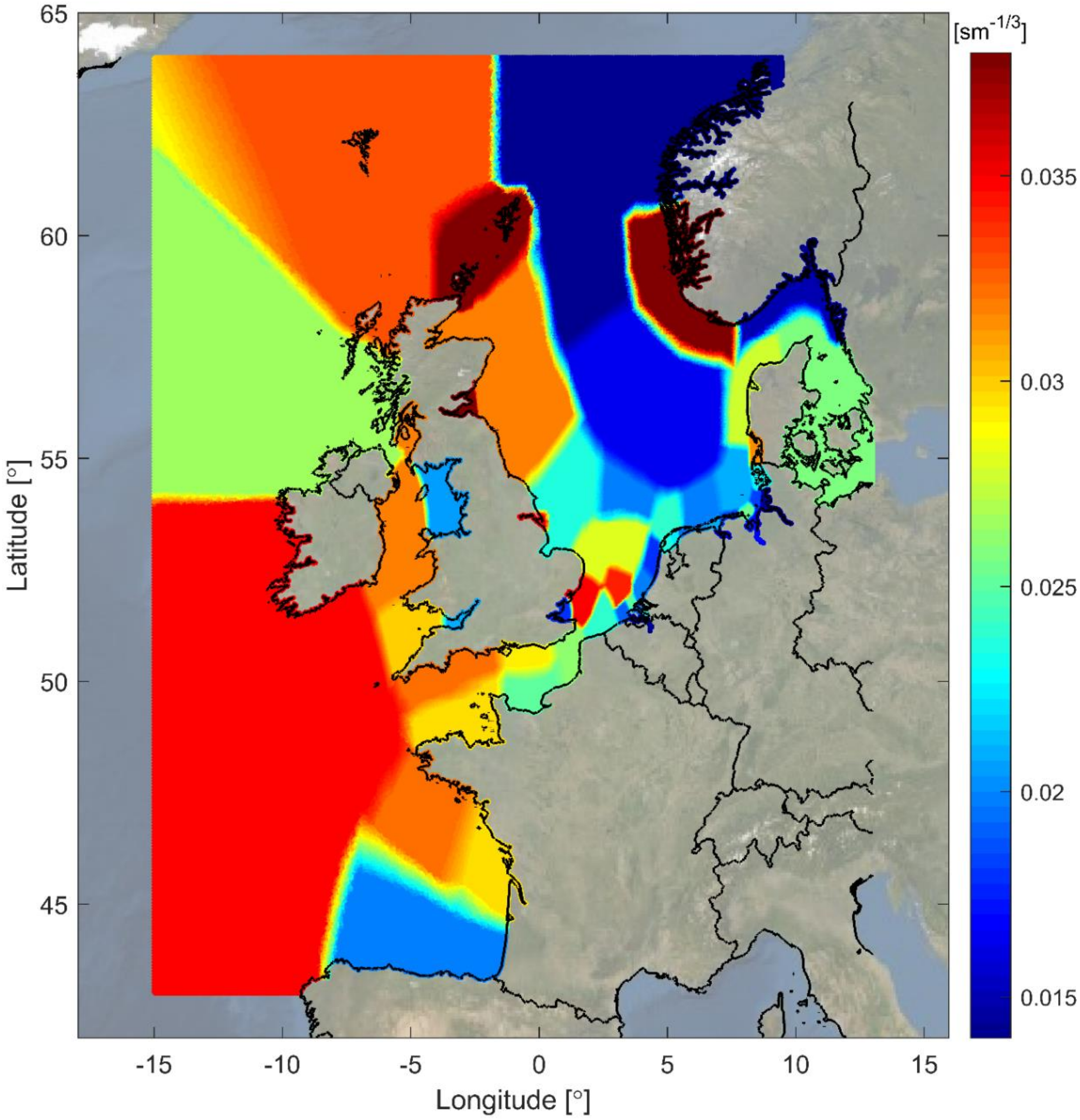

Figure 2.9 Overview of the space-varying Manning bottom roughness field of 3D DCSM-FM.

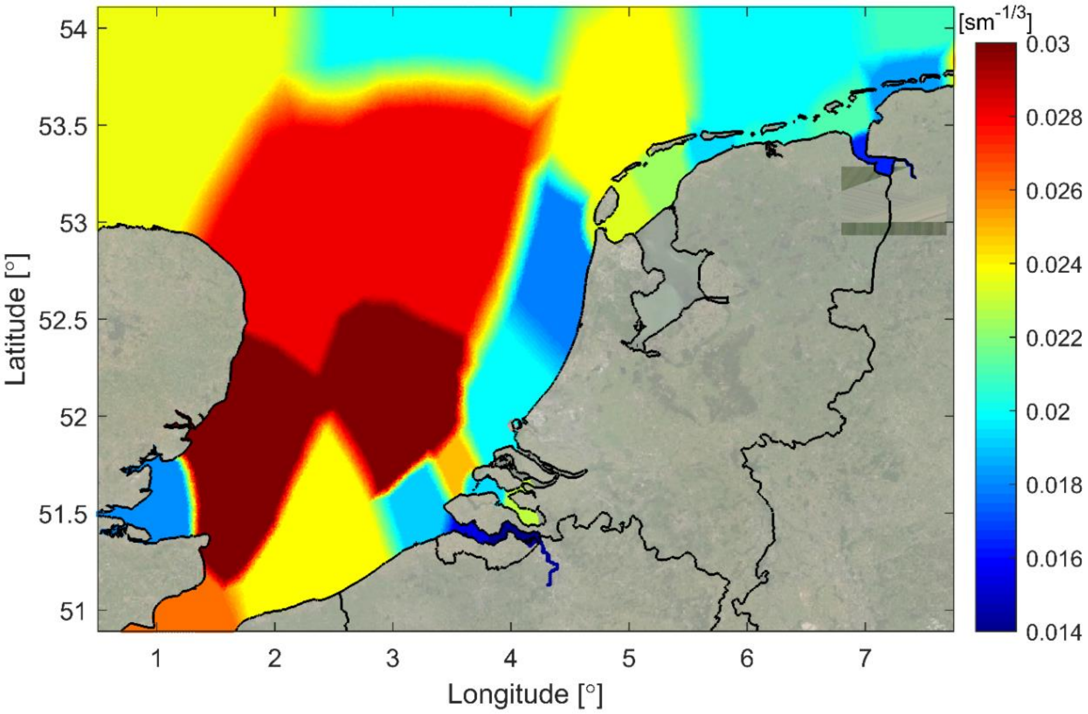

Figure 2.10 Detail of space-varying Manning bottom roughness field of 3D DCSM-FM in Dutch waters.

2.6 Open boundaries

Water levels

At the northern, western and southern and eastern open boundaries of 3D DCSM-FM, water level boundaries are applied. The eastern boundary is an addition compared to 2D DCSM-FM and is located in the western part of the Baltic Sea, just east of straits connecting it with the North Sea through the Kattegat and Skagerrak. Since these connections with the Baltic are very narrow, they have a limited impact on water levels in the North Sea, hence the closed boundary there in the 2D model. However, the Baltic Sea is an important source of fresh water transported towards and along the Norwegian North Sea coast, so it has been modelled as an open boundary in 3D DCSM-FM.

At the open boundary locations, astronomical water levels are imposed, derived from a harmonic expansion of the amplitudes and phase lags of 30 tidal constituents. These constituents are retrieved from the global tide model FES2012[2]. In contrast to the 2D barotropic model, the low-frequency constituents Sa (annual) and Ssa (semi-annual) have been disregarded, to avoid double-counting. These constituents are to a large extent baroclinic in nature, the effects of which are now explicitly modelled. In contrast to the 2D model, the diurnal S1 has not been adjusted, since processes governing this radiational tide are in principle included in this model.

[2] https://www.aviso.altimetry.fr/en/data/products/auxiliary-products/global-tide-fes/description-fes2012.html

Table 2.1 Overview of the tidal components prescribed at the open boundaries of 3D DCSM-FM, including their angular frequency (°/h).

Component name	Angular frequency (°/h)	Component name	Angular frequency (°/h)
MM	0.5443747	LABDA2	29.4556253
MF	1.0980331	NU2	28.5125831
MSF	1.0158958	L2	29.5284789
MFM	1.6424078	T2	29.9589333
Q1	13.3986609	S2	30.0000000
O1	13.9430356	R2	30.0410667
P1	14.9589314	K2	30.0821373
S1	15.0000000	M3	43.4761563
K1	15.0410686	N4	56.8794591
J1	15.5854433	M4	57.9682084
MNS2	27.4238337	MN4	57.4238337
2N2	27.8953548	MS4	58.9841042
MU2	27.9682084	S4	60.0000000
N2	28.4397295	M6	86.9523126
M2	28.9841042	M8	115.9364168

In the Delft3D FM software, the specified amplitudes and phases are converted into timeseries covering the required period by means of harmonic prediction. Implicitly it is assumed that the nodal cycle at the location of the open boundaries can be obtained from the equilibrium tide. The validity of this assumption is corroborated by Zijl (2016a).

The surge at the open boundaries is approximated by addition of an inverse barometer correction (IBC) to the astronomical water levels. This correction is a time- and space-dependent function of the local atmospheric pressure.

To account for steric (i.e. density driven) effects, the daily mean water levels from CMEMS[3] (product: GLOBAL_REANALYSIS_PHY_001_030) are used. In addition, an offset of +40 cm has been added to all boundaries. This value has been chosen such that it minimizes the M2 phase lag in a selection of stations along the Dutch coast.

Salinity and temperature
At the lateral open boundaries temperature and salinity are derived from CMEMS (product: GLOBAL_REANALYSIS_PHY_001_030). These daily values at 50 non-uniformly spaced vertical levels are interpolated by Delft3D Flexible Mesh to the right horizontal location and model layers.

2.7 Meteorological forcing

3D DCSM-FM has been coupled to ECMWF's ERA5 reanalysis dataset[4], which has a 0.25 degrees spatial resolution and hourly temporal resolution. The forcing parameters used are described below.

2.7.1 Momentum flux

To account for the air-sea momentum flux, time- and space-varying neutral wind speeds (at 10 m height) and atmospheric pressure (at MSL) are applied. With respect to air-sea momentum

[3] https://marine.copernicus.eu/
[4] https://www.ecmwf.int/en/forecasts/datasets/reanalysis-datasets/era5

exchange, the aim is to be consistent with the Atmospheric Boundary Layer (ABL) model that is used in the meteorological model applied. For coupling to ERA5 this implies using a Charnock formulation (Charnock, 1955) and specifying a time-and space-varying Charnock coefficient. The Charnock formulation assumes a fully developed turbulent boundary layer of the wind flow over the water surface. The associated wind speed profile follows a logarithmic shape.

In computing the wind shear stress, which represents the momentum exchange between air and water, the wind speed relative to the flow velocity at the water surface is used. While this implies less consistency with the ABL approximation in the meteorological model, this was proven to be beneficial to the quality with which water levels are represented (Zijl, 2016b).

2.7.2 Heat-flux

Horizontal and vertical spatial differences in water temperature affect the transport of water through its impact on the water density. For example, heating of surface water and shallow waters causes temperature gradients that can generate horizontal flow. It can also lead to temperature stratification with accompanying damping of turbulence and hence a reduction in vertical mixing. To include these effects, the transport of temperature is modelled. For its main driver, exchange of heat between the water surface and the atmosphere, a heat-flux model is used. This model considers the separate effects of solar (shortwave) and atmospheric (longwave) radiation, as well as heat loss due to back radiation, evaporation and convection. The temporally and spatially varying turbulent exchange of heat through the air-water interface, due to evaporation and convection, is computed based on the local temperature (at 2 m), dew point temperature and wind speed from the ERA5 meteorological reanalysis. To account for the radiative heat fluxes the surface net solar (short-wave) radiation and the surface downwelling long wave radiation have been imposed, while the surface upwelling long-wave radiation is computed based on the modelled sea surface temperature. The formulation for the latter component is specifically implemented in Delft3D FM for this model (although it has a general applicability). The incoming solar radiation is distributed over the water column, depending on the water transparency prescribed with a Secchi depth. In the hydrodynamic model a constant, uniform value of 4 m has been applied, except at the Wadden Sea, where this value is set to 1 m (reflecting enhanced concentrations of, for example, suspended sediment).

2.7.3 Mass-flux

To account for the mass-flux through the air-sea interface time- and space varying fields of evaporation and precipitation have been applied.

2.8 Freshwater discharges

Freshwater discharges in the 3D DCSM-FM domain are prescribed as sources with a climatological monthly mean discharge rate and associated water temperature based on data from E-HYPE.

The seven most important discharges in the Netherlands and three most important German rivers are replaced by gauged discharges with an hourly or daily interval. In periods where data is lacking, climatological monthly mean values are used. Due to the lack of river temperature data associated with the discharge gauges, a pragmatic approach was taken such that the temperature of the discharged water is based on nearby measurements of sea surface temperature, the location of which is presented in Table 2.2. Before being applied, the average seasonal temperature cycle is derived by fitting a sine function through the observed series. The salinity of all discharged water is assumed to be 0.01 psu[5].

An overview of the 847 discharge locations are shown in Figure 2.11. The locations in the Netherlands and in the German Bight are shown in more detail in Figure 2.12.

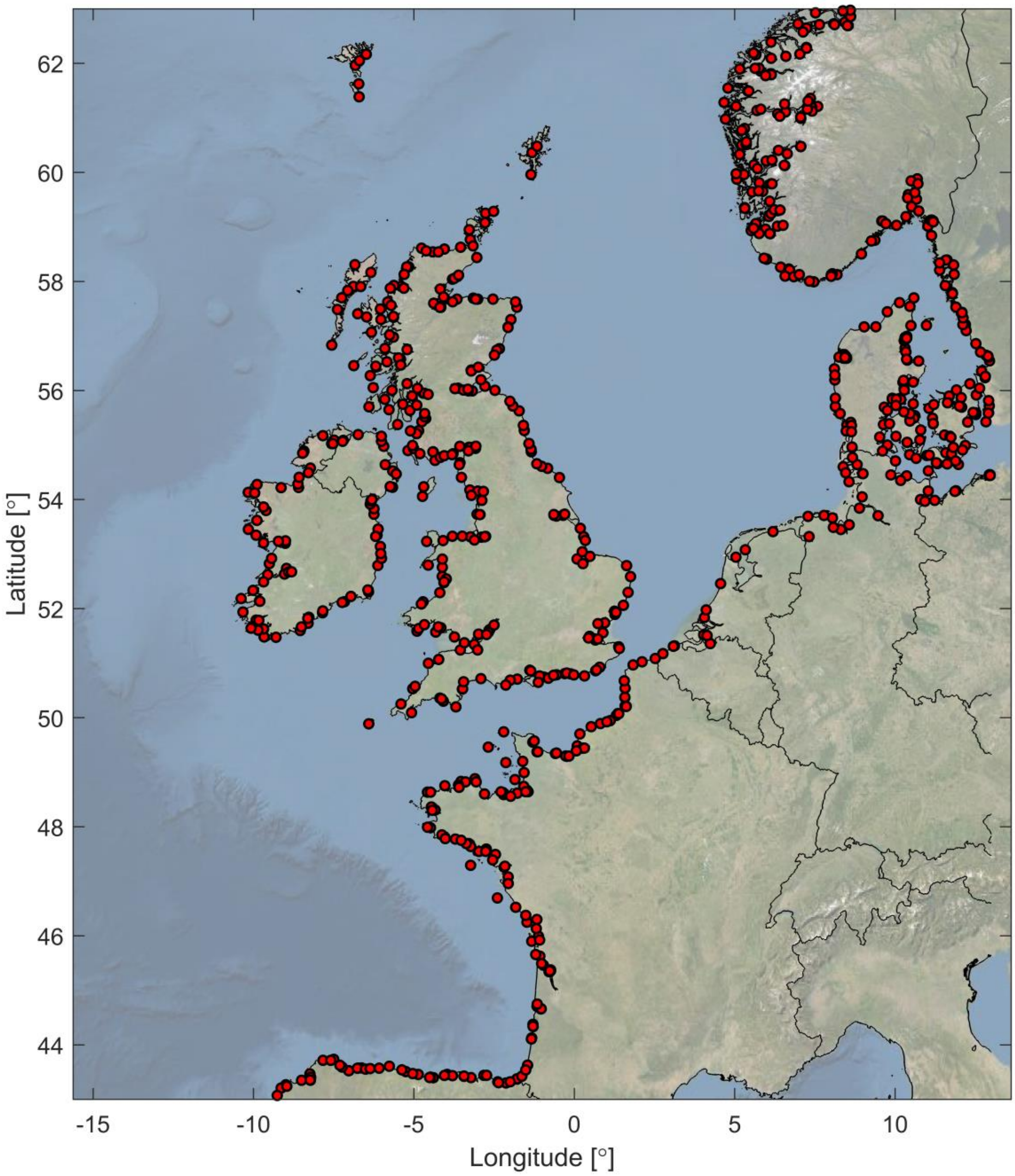

Figure 2.11 Overview of the discharge/river locations in 3D DCSM-FM

[5] It should be noted that this value may be quite low for the heavily populated European river basins. The sensitivity of the model results to a higher value will be examined in future versions of the model.

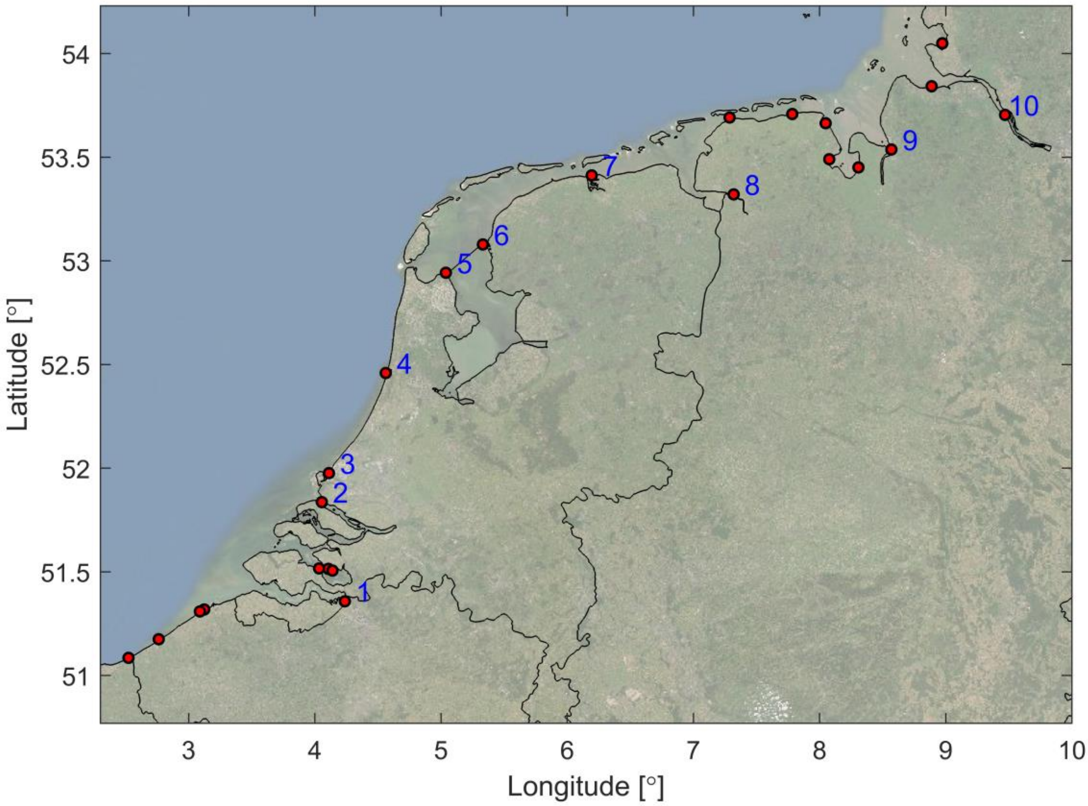

Figure 2.12 Overview of the discharge/river in 3D DCSM-FM located in the Netherlands. The station names that correspond with the numbers are listed in Table 2.2.

Table 2.2 Discharge/river names that are shown in Figure 2.12

#	Discharge/River name	Temperature based on station:
1	SCHAARVODDL	BAALHK
2	HARVSZBNN	HARVSS
3	MAASSS	HOEKVHLD
4	IJMDBNN	IJMDN1
5	DENOVBTN	DENOVR
6	KORNWDZBTN	KORNWDZBTN
7	Cleveringsluizen	SCHIERMNOG
8	Ems	DENOVR
9	Weser	DENOVR
10	Elbe	DENOVR

2.9 Miscellaneous

2.9.1 Tidal potential

The tidal potential representing the direct body force of the gravitational attraction of the moon and sun on the mass of water has been switched on. It is estimated that the effect of these Tide Generating Forces (TGF) has an amplitude in the order of 10 cm throughout the model domain. Components of the tide with a Doodson number from 55.565 to 375.575 have been included.

2.9.2 Horizontal turbulence

The horizontal viscosity is computed with the Smagorinsky sub-grid model, with the coefficient set to 0.20. The use of a Smagorinsky model implies that the viscosity varies in time and space and is dependent on the local cell size. With the exception of a two nodes wide strip along the open boundaries, a background value of 0.1 m^2/s is specified. Along the open boundaries a background value of 2000 m^2/s has been used.

2.9.3 Vertical turbulence

A k-ε turbulence closure model is used to compute the vertical eddy viscosity and diffusivity. In addition, a background value of 5×10^{-5} m^2/s is set for vertical eddy viscosity, which is a commonly used value to account for vertical transfer of momentum due to the presence of internal waves. For vertical eddy diffusivity, a background value of 2×10^{-5} m^2/s is used. This value has been determined after doing sensitivity simulations, comparing the modelled and measured vertical temperature difference (a measure of temperature stratification) at a location in the central North Sea.

2.9.4 Movable barriers

There are several movable barriers in the model area, such as the Thames Barrier, the Ems Barrier, the Eastern Scheldt Barrier and the Maeslant Barrier. These barriers protect the hinterland from flooding by closing in case high water is forecasted. The only barrier currently implemented in the model is the Eastern Scheldt Barrier.

The schematization of the three sections of the Eastern Scheldt Barrier on the model grid, are shown in green in Figure 2.13. In this figure, the red lines show the computational network, the red crosses illustrate the dry points (permanently inactive cells) and the thin dams are shown in yellow. The cross-sectional area of the barriers follows from a prescribed gate door height and width. These values are listed in Table 2.3. The width of each of the sections is the summed width of the individual gates in each section.

Table 2.3 Gate door height, width and sill height of the three sections of the Eastern Scheldt Barrier

Section	Gate door height [m]	Width [m]	Sill height [m MSL]
Schaar	11.27	916.40	-5.75
Hammen	11.63	859.13	-6.32
Roompot	14.11	1775.53	-8.60

The effect of the structures on the cross-sectional area at each of the structures is controlled by a timeseries of the gate lower edge level of the three sections (data provided by Rijkswaterstaat).

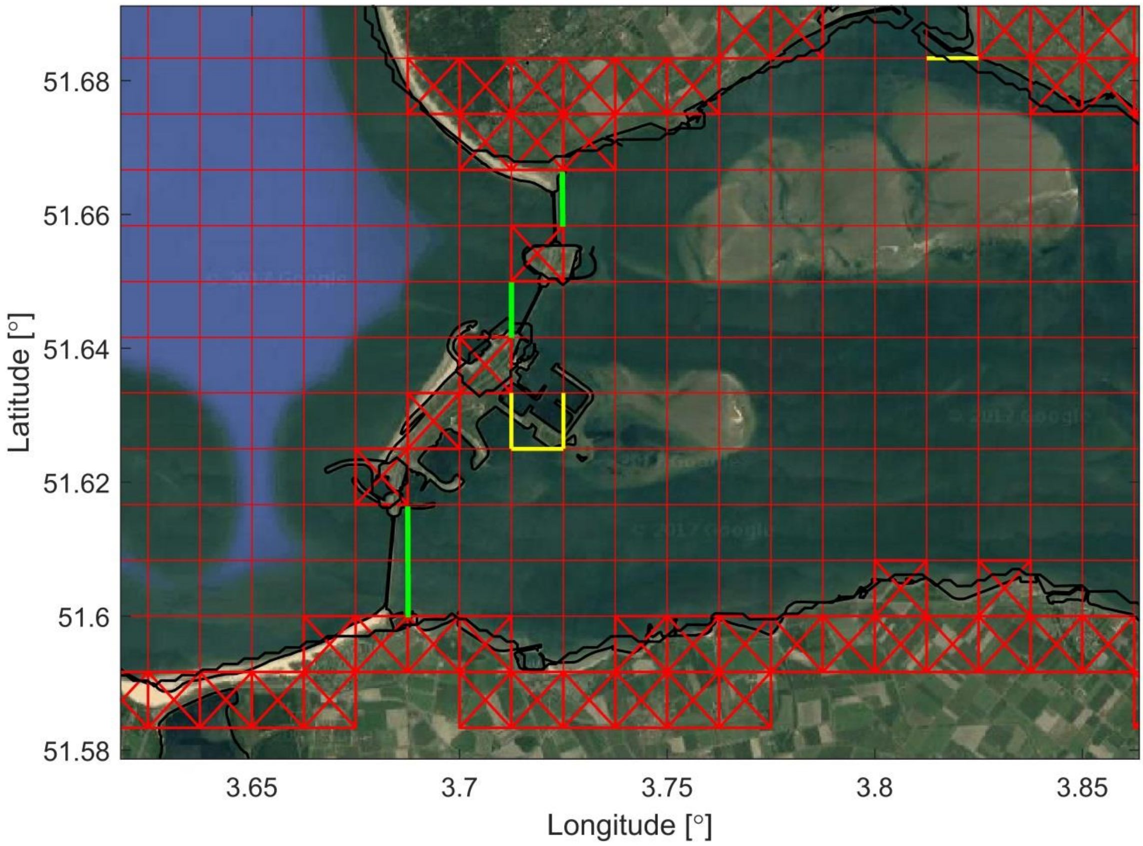

Figure 2.13 Implementation of the Eastern Scheldt Barrier in DCSM-FM (red lines: computational network; red crosses: dry points; yellow lines: thin dams; green lines: movable barriers).

2.9.5 Initial conditions and spin-up period

A uniform initial water level of zero elevation has been specified for the computations, while for the initial velocity, stagnant flow conditions have been prescribed. Salinity and temperature are initialized by interpolating the space-varying CMEMS data at the corresponding time to the 3D DCSM-FM horizontal and vertical grid. After starting from an external solution (CMEMS) with respect to temperature and salinity, a spin-up period of one year, forced by realistic lateral and surface (meteorological) boundary conditions and river discharge values, is applied to reach a dynamic equilibrium.

2.9.6 Time zone

The time zone of DCSM-FM is GMT+0 hr. This means that the phases of the harmonic boundary conditions and the tidal potential are prescribed relative to GMT+0 hr. As a result, the model output is in the same time zone.

2.9.7 Software version

3D DCSM-FM has been developed as an application of the D-Flow Flexible Mesh module (D-Flow FM) module of the Delft3D FM Suite. This module is suitable for one-, two-, and three-dimensional hydrodynamic modelling of free surface flows on unstructured grids. Various versions of D-Flow FM have been used during the development of 3D DCSM-FM. For the final validation presented in this report, use has been made of D-Flow FM version 1.2.100.66357 (Apr 10, 2020).

2.9.8 Numerical time step

D-Flow FM automatically limits the time step to prevent numerical instabilities. Since the computation of the advective term is done explicitly in D-Flow FM, the time step limitation is related to the Courant criterion. The maximum Courant number is set to 0.7. The maximum computational time step has been set to 2 minutes (120 s).

2.9.9 Computational time

Computations are performed on Deltares' h6 Linux-cluster (queue: codec) using 5 nodes with 4 cores each. With a maximum timestep of 120 s, and an average timestep of 110 s, this results in a computation time of 9.4 minutes per simulation-day (2.4 days per simulation-year).

In Table 2.4 the computational time of DCSM-FM is presented together with the (average) time step and cell size and the number of network nodes. This is done for both the 2D and 3D configuration of the model, with all computations performed on Deltares' h6 cluster using 5 nodes with 4 cores each.

Table 2.4 Overview of grid cell size, number of net nodes, maximum and average numerical time step and computational time for various 2D models. The computations were performed on Deltares' h6 cluster (queue: codec) using 5 nodes with 4 cores each.

Model	cell size (nm)	# nodes	Maximum time step (s)	Average time step (s)	Comp. time (min/day)	Comp. time (day/year)
2D DCSM-FM 0.5 nm	4nm-0.5nm	628,679	120	118.7	0.78	0.20
3D DCSM-FM	4nm-0.5nm	628,679	120	109.8	9.4	2.37

2.9.10 Comparison against default settings for D-HYDRO models

Table 2.5 provides an overview of the numerical and physical settings that deviate from the default settings that are advised to be used for sixth-generation model for Rijkswaterstaat (Minns et al., 2019). During the model setup and calibration, many numerical settings have been tested and discussed with the software developers. For each of the settings below, there is a substantiated reason to deviate the default value.

Table 2.5 Overview of default settings for D-HYDRO models and the deviating settings that are used in 3D DCSM-FM

Keyword	Default setting	3D DCSM-FM
BedlevUni	-5	5
OpenBoundaryTolerance	3	0.1
Newcorio	0	1
Corioadamsbashfordfac	0	0.5
Izbndpos	0	1
Tlfsmo	0	86400
Logprofkepsbndin	0	2
Keepzlayeringatbed	0	2
dicoww	5E-5	2E-5
TidalForcing	0	1
Secchi depth	2	4 (1 in Wadden Sea)
Stanton	-1	0.0013
Dalton	-1	0.0013
ICdtyp	2 (Smith and Banke)	4 (Charnock)

Relativewind	0	1
Rhoair	1.205	1.2265
PavBnd	0	101330
DtUser	300	600
DtMax	30	120
DtInit	1	60
Dxwuimin2D	0	0.1
Soiltempthick	1	0
RhoairRhowater	0	1
Jadelvappos	1	0
Dtfacmax	1.1	1.5

2.10 Differences with 2D DCSM-FM 0.5nm

In Table 2.6, a concise overview of the differences between 2D DCSM-FM 0.5nm and 3D DCSM-FM is presented.

Table 2.6 Overview of the differences between (2D) DCSM-FM 0.5nm and 3D DCSM-FM (0.5nm)

	2D DCSM-FM 0.5nm	3D DCSM-FM
Number of vertical layers	1	20 sigma-layers
Transport of salinity	excluded	included
Transport of temperature	excluded	included
Vertical turbulence	-	k-ε model
Spin-up period applied	10 days	~1 year
Baroclinic contribution to water level open boundary forcing	excluded	included
Tidal boundary forcing	32 constituents	30 constituents (Sa and Ssa excluded)
Open boundary locations	South, west and north	South, west and north and east (Baltic Sea boundary)
Meteorological forcing	Airpressure, windx, windy, charnock	Airpressure, windx, windy, charnock, dewpoint, airtemperature, cloudiness, solarradiation, longwaveradiation, rainfall, evaporation
Parametrization of energy dissipation by generation of internal waves	included	excluded
Increased horizontal background eddy viscosity and diffusivity along open boundary	Increased horizontal background eddy viscosity	Increased horizontal background eddy viscosity and diffusivity
River discharges (and associated salinity/ temperature)	excluded	included

3 Water level validation

3.1 Introduction

3.1.1 Quantitative evaluation measures (Goodness-of-Fit parameters)

3.1.1.1 Time series: total water level, tide and surge

To assess the quality of the computed water levels, the root-mean-square error (RMSE) is computed based on measured and computed total water levels for the entire 2013-2017 validation period. In addition, as it provides further insight in the origins of remaining errors, the tide and surge component are separated from the total water level (see section 3.1.2) and the quality of both tide and surge is assessed separately.

More information on the collection of water level data, the quality assurance procedure and the resulting dataset of tide gauge information can be found in Chapter 3 of the 2D DCSM-FM 0.5nm report (Zijl & Groenenboom, 2019).

3.1.1.2 High waters

The validation results were also assessed on the capacity to accurately hindcast peaks in water level, including the most extreme high waters in the validation period. Minor differences in timing between computed and measured high waters are less critical than a correct representation of the peak water level. Therefore, the vertical difference between each computed and measured high water (approximately twice a day) is computed and based on this, the error statistics can be determined. Measured and modelled high waters are matched if the difference in timing is less than 4 hrs.

The same can be done for the tidal signal derived from measured and modelled water levels, which yields the quality of the tidal high waters. What remains after subtracting these tidal high waters from the total high waters is called the skew surge, i.e. the difference between the peak water level and the astronomical peak. Note that the skew surge is generally lower than the highest ‘normal’ surge in the hours surrounding the high-water peak.

In addition, a subdivision is made between three categories of high-water events, based on the height of the measured skew surge:

- events with the 99% lowest skew surge heights,
- events with skew surge heights between 99.0% and 99.8%
- the highest 0.2% skew surges

The latter category represents storm conditions yielding the most extreme skew surge conditions observed in the years 2013-2017. If measurements are complete, this category consists of 8 values, while the first two categories then contain 3492 and 28 values, respectively.

For the total high waters, tidal high-waters and skew surge, the bias, standard deviation (std) and RMSE are determined for each of these categories.

3.1.1.3 Mean water level

The water levels computed with 3D DCSM-FM (or any other hydrodynamic model) refer to an equipotential surface of the Earth's gravity field. Gradients in baroclinic pressure (i.e. due to density differences) affect the movement of water and can, consequently, affect the long-term mean water level (or Mean Dynamic Topography). In assessing 2D models, such as 2D DCSM-FM 0.5nm, the bias between measured and computed water levels in each station, determined over the entire five-year validation period, is usually disregarded in the Goodness-of-Fit criteria used. This is because the density in these models is assumed to be constant and uniform. Also, while tide and surge caused by variations in atmospheric pressure are accounted for at the open boundaries, steric effects (i.e., changes in sea level due to thermal expansion and salinity variations) are not, which affects the ability to represent the mean water level field.
A 3D model including transport of salinity and temperature is in principle capable to represent these phenomena, and therefore also the Mean Dynamic Topography. Nonetheless, the same approach as for assessing 2D models (i.e., removing the bias first) is also used here, since this approach removes the need to convert all measurements to a uniform vertical reference plane that is valid for the entire model domain. Disregarding the bias is achieved by correcting the measurements for this bias before these criteria are determined. Consequently, when considering the entire period, the Root-Mean-Square (RMS) of the error signal is equal to the standard deviation thereof.

3.1.2 Harmonic analysis

The separation of the tide and surge contribution to the total water level is done by means of harmonic analysis using the MATLAB package t_tide (Pawlowicz et al. 2002). After obtaining the tide through harmonic analysis and prediction, the surge (or ‘non-tidal residual’) is obtained by subtracting the predicted tide from the total water level signal. Since the 18.6-year nodal cycle is assumed to be constant in the harmonic analysis, we restricted the analysis period to one year. This implies that for each year in the 5-year validation period, the harmonic analysis is performed. Harmonic analysis is only performed when the completeness index of the measurements is larger than 80% and the length of the available measurements within the analysis period is larger than 300 days.

Based on the possibility to separate constituents using a time series of one year, 118 constituents have been selected to be used in the harmonic analysis. Note that the number of constituents used here is much larger than the number of constituents prescribed on the open boundaries of the model (cf. Table 3.1). This is because many more shallow water constituents, such as compound tides and overtides, are generated inside the model domain, especially in shallow areas where non-linear processes become important. At the location of the open boundaries the amplitudes of these additional constituents are generally assumed to be negligible.

Table 3.1 List of harmonic constituents used for harmonic analysis

Component name	Angular frequency (°/h)	Component name	Angular frequency (°/h)
SA	0.0410667	3MS4	56.9523127
SSA	0.0821373	MN4	57.4238338
MSM	0.4715211	ST9	57.5059711
MM	0.5443746	ST40	57.8860712
MSF	1.0158958	M4	57.9682085
MF	1.0980330	ST10	58.0503457
ALP1	12.3827652	SN4	58.4397296
2Q1	12.8542863	KN4	58.5218669

SIG1	12.9271398	MS4	58.9841042
Q1	13.3986609	MK4	59.0662415
RHO1	13.4715145	SL4	59.5284789
O1	13.9430356	S4	60.0000000
TAU1	14.0251729	SK4	60.0821373
BET1	14.4145567	MNO5	71.3668694
NO1	14.4966940	2MO5	71.9112441
CHI1	14.5695475	MNK5	72.4649025
PI1	14.9178647	2MP5	72.9271398
P1	14.9589314	2MK5	73.0092771
S1	15.0000020	MSK5	74.0251729
K1	15.0410686	2SK5	75.0410686
PSI1	15.0821353	ST11	85.4013260
PHI1	15.1232059	2NM6	85.8635634
THE1	15.5125897	ST12	85.9457007
J1	15.5854433	2MN6	86.4079380
SO1	16.0569644	ST13	86.4900753
OO1	16.1391017	ST41	86.8701754
UPS1	16.6834763	M6	86.9523127
2NS2	26.8794591	MSN6	87.4238338
ST37	26.9523127	MKN6	87.5059711
OQ2	27.3509802	2MS6	87.9682085
EPS2	27.4238338	2MK6	88.0503458
ST2	27.5059711	NSK6	88.5218669
2N2	27.8953549	2SM6	88.9841042
MU2	27.9682085	MSK6	89.0662415
N2	28.4397296	ST16	101.9112441
NU2	28.5125831	3MK7	101.9933814
OP2	28.9019670	ST18	114.8476676
H1	28.9430376	3MN8	115.3920423
M2	28.9841043	ST19	115.4741796
H2	29.0251709	M8	115.9364170
MKS2	29.0662415	ST20	116.4079381
LDA2	29.4556253	ST21	116.4900753
L2	29.5284789	3MS8	116.9523127
T2	29.9589333	3MK8	117.0344500
S2	30.0000000	ST22	117.5059711
R2	30.0410667	ST23	117.9682085
K2	30.0821373	ST24	118.0503458
MSN2	30.5443747	ST26	130.4331109
ETA2	30.6265119	4MK9	130.9774856
2SM2	31.0158958	ST27	131.9933813
SKM2	31.0980330	ST28	144.3761465
NO3	42.3827652	M10	144.9205212
MO3	42.9271398	ST29	145.3920423
M3	43.4761564	ST30	145.9364170
SO3	43.9430356	ST31	146.4900753
MK3	44.0251729	ST32	146.9523127
SK3	45.0410687	M12	173.9046254

ST8	56.4079380	ST34	174.9205212
N4	56.8794591	ST35	175.4741796

3.2 Shelf-wide results

A spatial overview of the RMSE-values of the total water level, tide and surge of all shelf-wide tide gauge stations is given in Figure 3.1 and Figure 3.2 (left- and right-hand side panel), respectively.

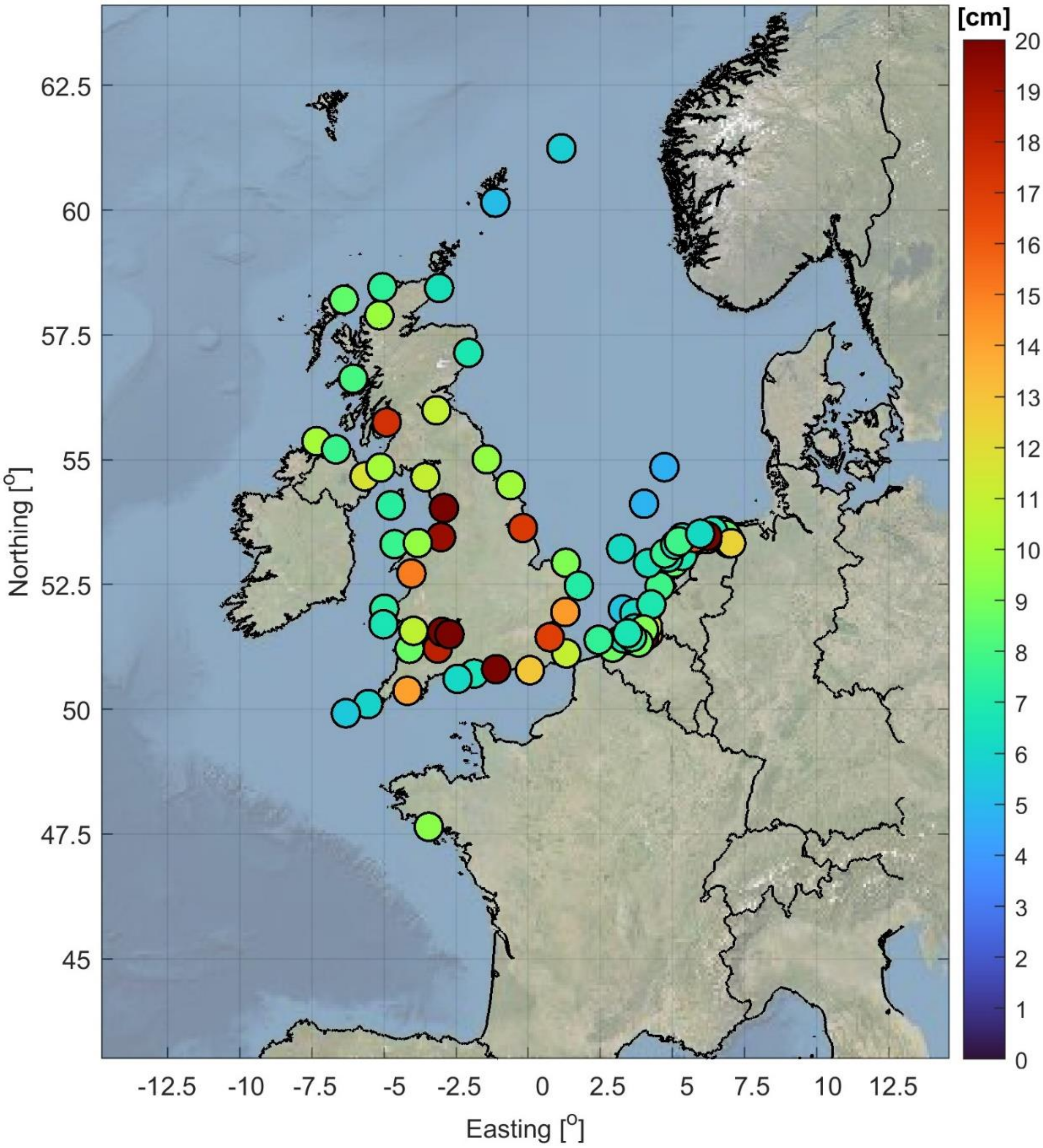

Figure 3.1 Spatial overview of the RMSE-values (cm) of the total water level for the period 2013-2017 of all shelf-wide tide gauge stations

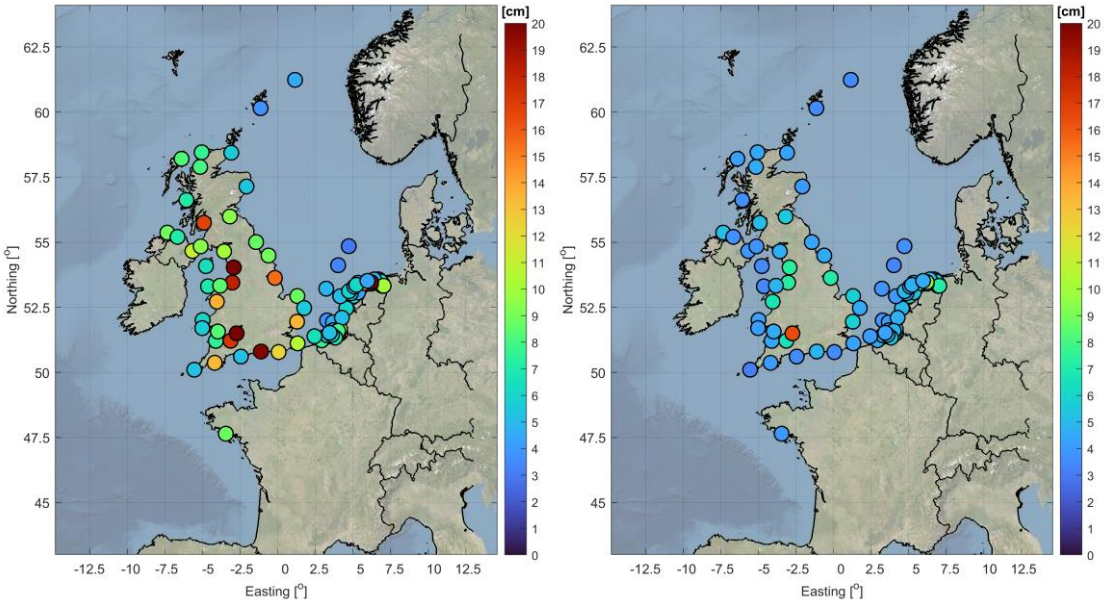

Figure 3.2 Spatial overview of the RMSE-values (cm) of the tide (left panel) and surge (right panel) for the period 2013-2017 of all shelf-wide tide gauge stations

The mean model skill in terms of RMSE for the tide, surge and total water level for all shelf-wide tide gauge stations is summarized in Table 3.2. Note that the average statistics for tide are influenced by a few coastal stations affected by lack of accurate representation of local geometry and bathymetry features, due to a comparatively course resolution relative to the relevant local spatial scales.

Table 3.2 Mean statistics (RMSE in cm) of the tide, surge and total water level for the period 2013-2017 of all shelf-wide tide gauge stations

Stations	**RMSE tide (cm)**	**RMSE surge (cm)**	**RMSE water level (cm)**
Shelf-wide	9.1	5.2	10.7

The numbers for the RMSE of tide, surge and total water level for all shelf-wide tide gauge stations, can be found in Appendix A.1.1.

3.3 Dutch coastal waters

3.3.1 Observation stations

For further analysis of the results, the emphasis will be on a set of 37 Dutch coastal stations with two nearby Belgian and four German stations added. A list of these 43 stations is presented in Table 3.3, in order of increasing M2 phase lag. To further aid analysis of the model quality, a sub-division is also made in four different sets of stations: 16 stations along the North Sea coast, 5 offshore stations (more than 10-15 km from coast), 6 stations in the Eastern and Western Scheldt and 16 stations in the Wadden Sea and Ems-Dollard.

Compared to the set of observations stations used within the validation of 2D DCSM-FM 0.5nm, stations Wandelaar and Zeebrugge_Leopolddam are not included in the current set.

Table 3.3 Names of the tide gauge stations used for quantitative model evaluation in Dutch coastal waters. Some Belgian and German stations nearby have been added, indicated here with BE and DE, respectively. The stations are further subdivided in four groups: coast, offshore, south-western delta (SWD) and Wadden Sea (incl. Ems-Dollard)

1	Bol van Heist (BE)	coast	23	K13a Platform	offshore
2	Scheur Wielingen (BE)	coast	24	F16	offshore
3	Cadzand	coast	25	Oudeschild	Wadden Sea
4	Westkapelle	coast	26	Den Oever Buiten	Wadden Sea
5	Europlatform	offshore	27	Terschelling Noordzee	coast
6	Vlissingen	SWD	28	Vlieland Haven	Wadden Sea
7	Roompot Buiten	coast	29	West-Terschelling	Wadden Sea
8	Lichteiland Goeree	offshore	30	Kornwerderzand Buiten	Wadden Sea
9	Brouwershavense Gat 08	coast	31	Wierumergronden	coast
10	Terneuzen	SWD	32	Huibertgat	coast
11	Haringvliet 10	coast	33	Harlingen	Wadden Sea
12	Hansweert	coast	34	Nes	Wadden Sea
13	Roompot Binnen	SWD	35	Lauwersoog	Wadden Sea
14	Hoek van Holland	coast	36	Schiermonnikoog	Wadden Sea
15	Stavenisse	SWD	37	Borkum Sudstrand (DE)	Wadden Sea
16	Berge Diepsluis West	SWD	38	Borkum Fischerbalje (DE)	Wadden Sea
17	Krammerssluizen West	SWD	39	Emshorn (DE)	Wadden Sea
18	Scheveningen	coast	40	Eemshaven	Wadden Sea
19	IJmuiden Buitenhaven	coast	41	Dukegat	Wadden Sea
20	Platform Q1	offshore	42	Delfzijl	Wadden Sea
21	Den Helder	coast	43	Knock (DE)	Wadden Sea
22	Texel Noordzee	coast			

3.3.2 Total water levels, tide and surge

3.3.2.1 3D DCSM-FM

A spatial overview of the RMSE-values of the total water level, tide and surge of the Dutch coastal stations is presented in Figure 3.3 and Figure 3.4 (left- and right-hand side panel), respectively. Generally, the total water level RMSE is 6-8 cm in North Sea waters. In these stations, the tide and surge RMSE is generally 4-6 cm. The quality deteriorates inside the Dutch estuaries and Wadden Sea, where the model resolution is low compared to the variability in geometry and bathymetry. This is especially noticeable in the eastern Wadden Sea (including the Ems-Dollard estuary) and the eastern part of the Eastern Scheldt where tidal channels are too narrow to properly represent on the model network. The result is a poor representation of the tide, while some impact is also noticeable in the surge quality, presumably due to a poor representation of the non-linear tide-surge interaction.

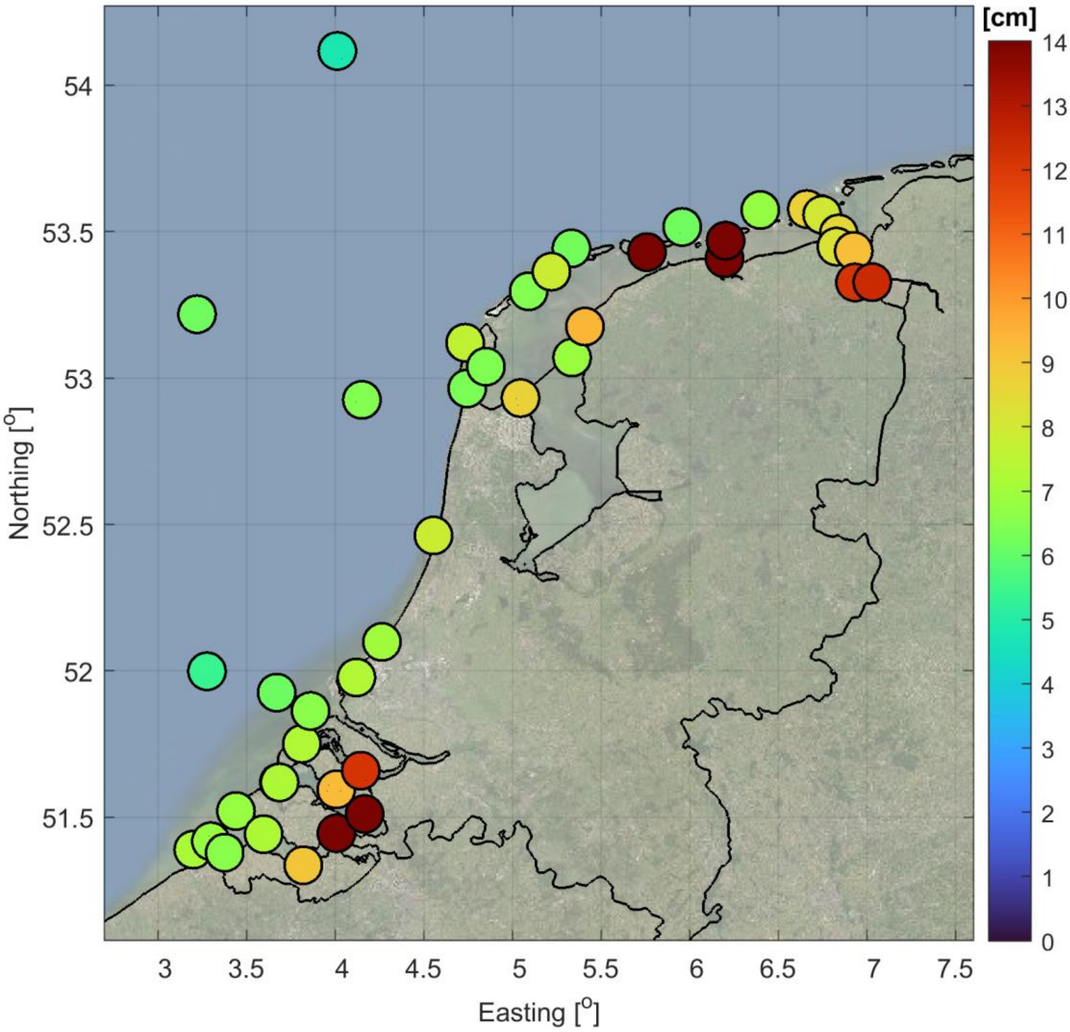

Figure 3.3 Spatial overview of the RMSE-values (cm) of the total water level for the period 2013-2017 of the Dutch coastal stations

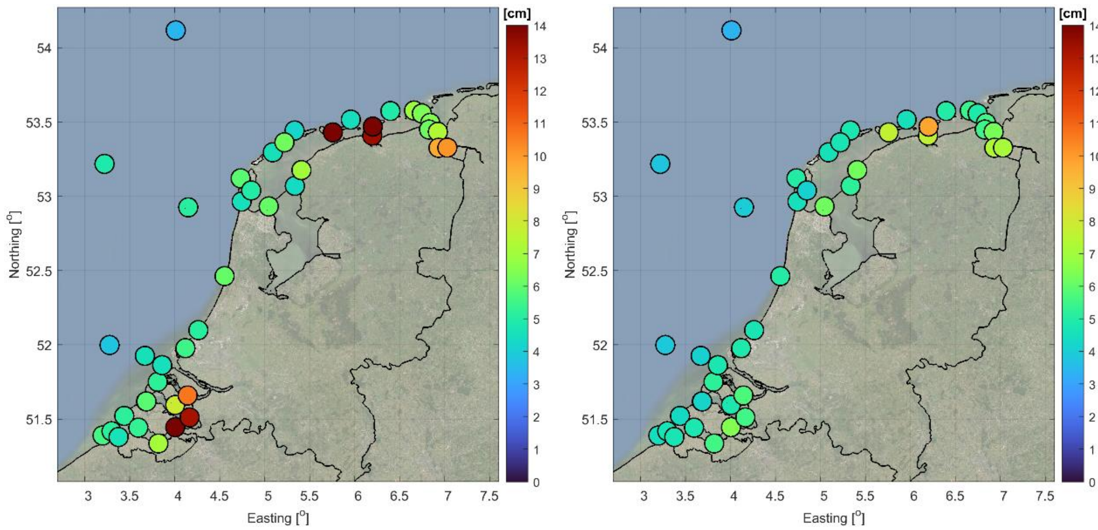

Figure 3.4 Spatial overview of the RMSE-values (cm) of the tide (left panel) and surge (right panel) for the period 2013-2017 of the Dutch coastal stations

3.3.2.2 Comparison against 2D DCSM-FM 0.5nm

As the 2D DCSM-FM 0.5 nm schematisation (as reported in Zijl & Groenenboom (2019)) uses meteorological forcing from KNMI's HiRLAM and 3D DCSM-FM is forced with meteorological data from ECMWF's ERA5-dataset, an additional simulation (2D DCSM-FM 0.5nm with ERA5-meteo-forcing) is performed to allow for a fair comparison between the 2D- and 3D DCSM-FM schematisations. When not indicated, the 2D DCSM-FM 0.5nm version is the simulation that is (in agreement with 3D DCSM-FM) forced with ERA5-data.

Table 3.4 shows the RMSE of tide, surge and total water level in Dutch coastal stations, for 3D DCSM-FM, in comparison to the depth-averaged DCSM-FM 0.5nm (with meteorological forcing HiRLAM and ERA5). A similar table, but for all shelf-wide tide gauge stations, together with the statistics of 2D DCSM-FM 0.5nm (with HiRLAM- and ERA5-forcing), can be found in Appendix A.1.1. A spatial overview of the absolute and percentage difference in RMSE (3D DCSM-FM minus 2D DCSM-FM 0.5nm), for both total water level, tide and surge, is illustrated in Figure 3.5 to Figure 3.7.

The difference in RMSE of tide, surge and total water level for the individual stations of the depth-averaged 2D DCSM-FM 0.5nm forced with either meteorological data from HiRLAM or ERA5 is only a few millimetres. The model forced with ERA5-data results in an (station-averaged) improvement of the computed surge. As the RMSE of the tidal component deteriorates, the RMSE of the total water level is quite similar.

The comparison of 3D DCSM-FM against 2D DCSM-FM 0.5nm (ERA5) shows that the quality of the representation of the tide is, averaged over all Dutch coastal stations, very similar (5.0 cm vs. 5.1 cm). The RMSE of tide averaged over the stations within the south-western delta (SWD) increases with 1 cm. This is caused by a deterioration of the predicted tides in the Eastern Scheldt. In all subsets, the RMSE of the modelled surge of 3D DCSM-FM is decreased by approximately 0.5 cm. Averaged over all stations considered here, the surge RMSE decreases from 5.8 cm to 5.2 cm, a 10% reduction. With respect to total water levels, the 3D model results appear to be slightly better than the 2D model results, with the average RMSE decreasing from 9.2 cm to 8.9 cm.

Table 3.4 Statistics (RMSE in cm) of tide, surge and total water level of 2D DCSM-FM 0.5nm (with meteorological forcing HiRLAM and ERA5) and 3D DCSM-FM for the Dutch coastal stations. The main locations (Dutch: 'hoofdlocaties') are shown in bold.

Station	RMSE tide (cm)			RMSE surge (cm)			RMSE water level (cm)		
	2D DCSM-FM 0.5nm (HiRLAM)	2D DCSM-FM 0.5nm (ERA5)	3D DCSM-FM 0.5nm	2D DCSM-FM 0.5nm (HiRLAM)	2D DCSM-FM 0.5nm (ERA5)	3D DCSM-FM 0.5nm	2D DCSM-FM 0.5nm (HiRLAM)	2D DCSM-FM 0.5nm (ERA5)	3D DCSM-FM 0.5nm
Bol_Van_Heist	5.5	5.5	5.6	5.2	5.1	4.4	7.5	7.5	7.2
Scheur_Wielingen_B.	5.7	5.6	5.1	5.4	5.2	4.6	7.7	7.5	6.8
CADZD	5.8	5.7	4.6	5.7	5.6	4.7	8.1	8.0	6.6
WESTKPLE	6.3	6.2	5.2	5.1	5.1	4.3	8.1	8.0	6.8
EURPFM	3.7	3.7	3.8	4.7	4.4	3.8	5.8	5.6	5.4
VLISSGN	6.3	6.3	5.4	5.6	5.6	4.8	8.4	8.5	7.2
ROOMPBTN	3.8	3.9	4.5	5.0	4.9	4.4	6.3	6.3	6.2
LICHTELGRE	4.7	4.8	4.6	4.7	4.4	4.1	6.7	6.5	6.1
BROUWHVSGT08	6.1	6.1	5.2	6.1	6.0	5.2	8.5	8.5	7.3
TERNZN	6.7	7.0	7.1	6.2	6.3	5.5	9.1	9.4	9.0
HARVT10	4.3	4.4	4.5	5.4	5.0	4.8	6.9	6.7	6.6
HANSWT	18.9	19.2	19.3	7.1	7.3	6.5	20.2	20.5	20.4

ROOMPBNN	4.4	4.5	5.9	4.9	4.8	4.2	6.6	6.6	7.2
HOEKVHLD	4.4	4.7	5.5	5.8	5.4	4.9	7.3	7.1	7.3
STAVNSE	5.5	5.7	7.9	5.4	5.4	4.9	7.7	7.9	9.3
BERGSDSWT	11.0	11.3	13.2	6.2	6.0	5.6	12.6	12.8	14.3
KRAMMSZWT	8.1	8.4	10.7	6.3	6.3	5.7	10.2	10.5	12.1
SCHEVNGN	4.5	4.7	5.1	5.6	5.3	4.7	7.1	7.0	6.9
IJMDBTHVN	5.4	5.6	6.1	5.8	5.6	5.0	7.9	7.9	7.9
Q1	4.2	4.4	5.1	4.6	4.5	4.0	6.3	6.3	6.5
DENHDR	4.2	4.4	4.5	5.1	5.1	4.5	6.6	6.7	6.4
TEXNZE	5.0	5.1	5.9	5.6	5.4	5.0	7.4	7.3	7.6
K13APFM	4.3	4.5	4.9	4.4	4.2	3.8	6.1	6.1	6.2
F16	3.0	3.3	3.4	4.1	3.9	3.4	5.0	5.2	4.8
OUDSD	4.6	4.8	5.0	4.7	4.6	4.1	6.6	6.6	6.5
DENOVBTN	7.4	7.8	6.0	6.9	6.6	6.2	10.1	10.2	8.7
TERSLNZE	4.4	4.4	4.2	5.6	5.4	4.8	7.1	6.9	6.3
VLIELHVN	3.8	4.1	4.6	5.0	5.0	4.5	6.3	6.4	6.5
WESTTSLG	4.8	5.0	6.2	5.0	4.9	4.7	7.0	7.0	7.8
KORNWDZBTN	4.6	4.9	4.4	5.7	5.3	5.2	7.3	7.2	6.9
WIERMGDN	4.8	4.7	4.4	5.5	5.1	4.5	7.2	6.9	6.2
HUIBGT	5.2	5.0	5.0	5.7	5.3	5.0	7.5	7.0	6.7
HARLGN	8.7	8.8	7.0	6.8	6.5	6.3	11.0	10.9	9.4
NES	15.4	15.4	14.1	7.6	8.0	7.6	17.2	17.4	16.0
LAUWOG	14.2	14.1	13.4	7.5	7.6	7.6	16.0	16.1	15.4
SCHIERMNOG	24.2	24.4	23.6	9.9	10.1	9.8	26.1	26.3	25.6
BORKUM_Sudstrand	7.3	7.3	6.9	5.7	5.7	5.4	9.2	9.3	8.7
BorkumFischerbalje	6.7	6.7	6.4	5.7	5.5	4.9	8.8	8.6	8.0
EMSHORN	7.6	7.4	6.4	6.1	6.2	5.6	9.7	9.6	8.5
EEMSHVN	7.2	7.0	6.1	6.2	6.1	5.5	9.5	9.2	8.2
DUKEGAT	8.0	7.8	7.3	7.0	6.8	6.3	10.1	9.9	9.2
DELFZL	10.8	10.5	9.7	7.9	7.9	7.3	13.4	13.2	12.1
KNOCK	11.0	10.7	10.1	7.7	7.8	7.1	13.4	13.2	12.4
Average (total)	7.0	7.1	7.1	5.9	5.8	5.2	9.2	9.2	8.9
Average (offshore)	4.0	4.1	4.4	4.5	4.3	3.8	6.0	5.9	5.8
Average (coast)	5.0	5.1	5.0	5.5	5.3	4.7	7.4	7.3	6.9
Average (SWD)	8.7	8.9	9.9	5.9	6.0	5.3	10.7	10.9	11.4
Average (WS)	9.1	9.2	8.6	6.6	6.5	6.1	11.4	11.3	10.6

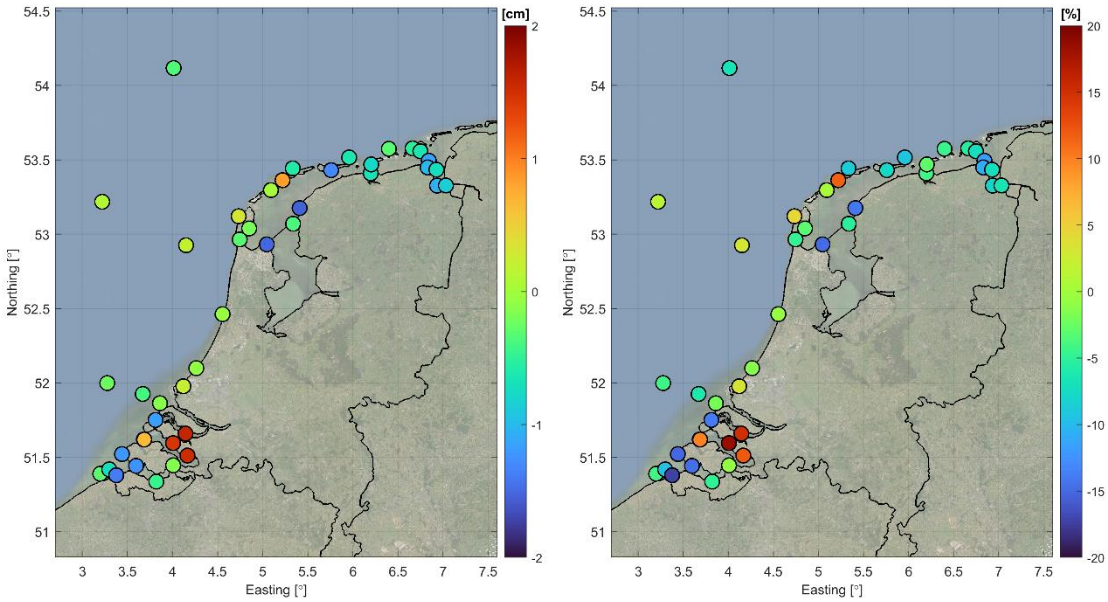

*Figure 3.5 Spatial overview of the difference (3D DCSM-FM minus 2D DCSM-FM 0.5nm) in RMSE of the **total water level** for the period 2013-2017 of the Dutch coastal stations. Left: difference (cm); right: relative difference (%).*

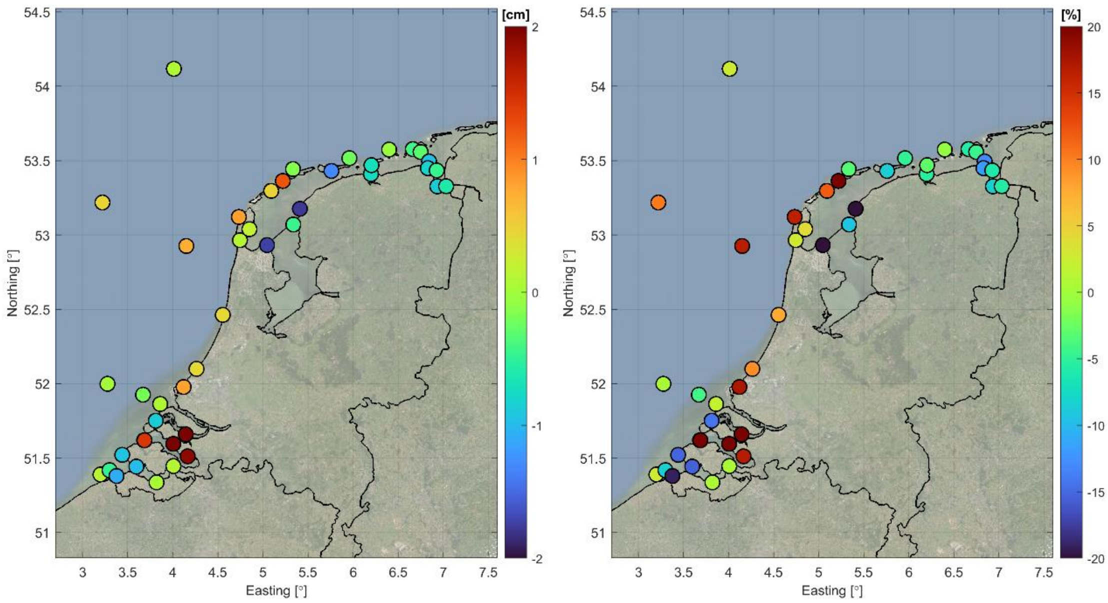

*Figure 3.6 Spatial overview of the difference (3D DCSM-FM minus 2D DCSM-FM 0.5nm) in RMSE of the **tide** for the period 2013-2017 of the Dutch coastal stations. Left: difference (cm); right: relative difference (%).*

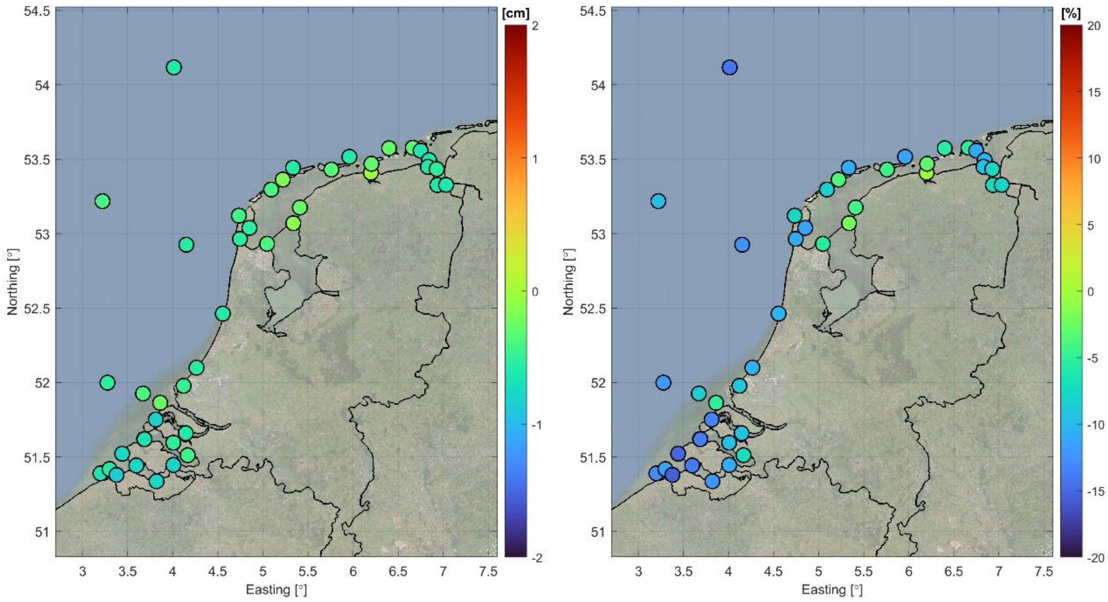

Figure 3.7 Spatial overview of the difference (3D DCSM-FM minus 2D DCSM-FM 0.5nm) in RMSE of the ***surge*** *for the period 2013-2017 of the Dutch coastal stations. Left: difference (cm); right: relative difference (%).*

3.3.2.3 Comparison against ZUNO-DD Water levels

The quality of the water level representation in the year 2014 has been determined in terms of the root-mean-square error (RMSE) and presented in Table 3.5. For these Dutch coastal stations, the average total water level RMSE is 7.0 cm. This result is significantly better than that of the previous generation 3D ZUNO-DD model of the southern North Sea (25.6 cm) , which is due to substantial improvements in both tide and surge.

Table 3.5 Comparison of water level representation (RMSE, determined for 08-01-2014 to 01-01-2015) between ZUNO-DD and 3D DCSM-FM (0.5 nm), for tide, surge and total water level signal.

	RMSE tide (cm)			RMSE surge (cm)			RMSE water level (cm)		
Station	ZUNO-DD	3D DCSM-FM	%	ZUNO-DD	3D DCSM-FM	%	ZUNO-DD	3D DCSM-FM	%
Cadzand	30.5	5.0	-84%	13.1	4.3	-67%	33.2	6.6	-80%
Westkapelle	27.0	5.8	-79%	12.7	4.2	-67%	29.9	7.2	-76%
Haringvliet 10	21.1	4.5	-79%	11.9	4.5	-62%	24.3	6.4	-74%
Hoek van Holland	17.1	5.5	-68%	11.8	4.8	-59%	20.7	7.3	-65%
Scheveningen	19.5	5.0	-74%	12.0	4.5	-63%	22.9	6.8	-70%
IJmuiden Buitenhav.	18.7	6.0	-68%	12.2	4.9	-60%	22.4	7.7	-66%
Average	22.3	5.3	-76%	12.3	4.5	-63%	25.6	7.0	-73%

3.3.3 Tide (frequency domain)

3.3.3.1 Amplitude and phase error of the M2-component

Figure 3.8 illustrates the amplitude and phase error of the M2-component, respectively. These results show that generally, in stations not hampered by a poor model resolution, the amplitude error is less than 3 cm, while the phase error is less than 2°.

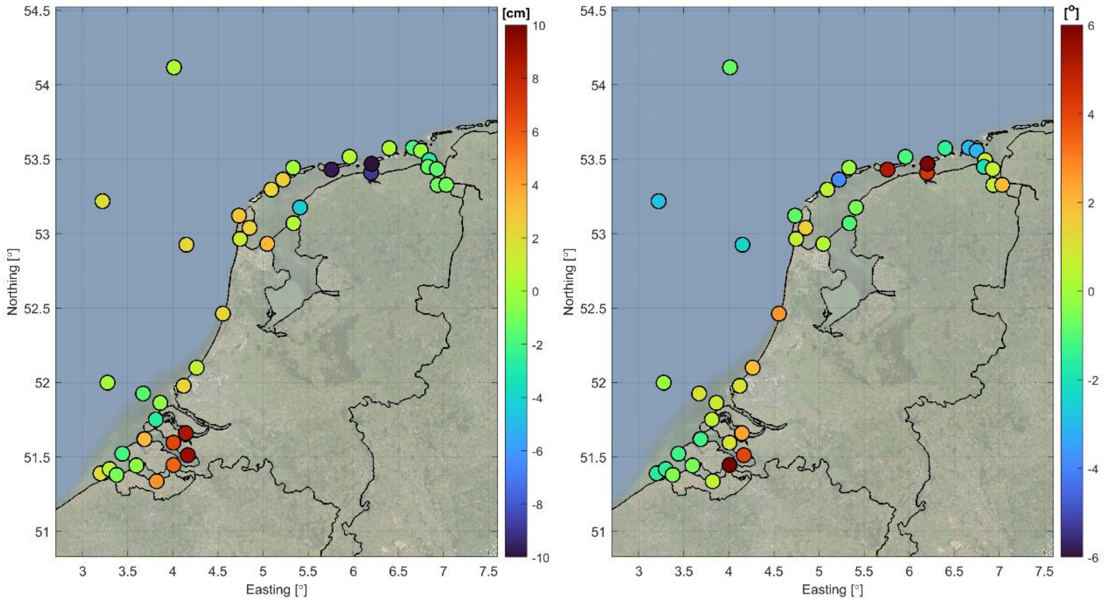

Figure 3.8 Spatial overview of the amplitude error (cm; left) and phase error (º) of the M2-component

3.3.3.2 Contribution of harmonic components to tidal error

In Table 3.6 an overview is given of the errors in the 10 harmonic constituents with the largest contribution to the tidal error in the subset 'coastal stations' (see Table 3.3) of both the depth-averaged DCSM-FM 0.5nm and 3D DCSM-FM.

The solar annual constituent Sa is the largest contributor to the tidal error of 3D DCSM-FM. In 2D DCSM-FM 0.5nm the Sa annual cycle was added along the open boundaries as a barotropic signal, even though the phenomenon is to a large extent baroclinic in nature. In 3D DCSM-FM, this annual cycle should follow from the physics resolved in the model. The reduced accuracy in the 3D model is presumably caused by a poor representation of the summer sea surface temperature in deep, oceanic waters. To properly resolve this relatively thin layer of warm surface water, a different vertical layer distribution is required. It is recommended to improve this in future updates of this the model.

Surprisingly, the contribution of M2 to the total tidal error in 3D DCSM-FM is less than in 2D DCSM-FM 0.5nm where the bottom roughness has been calibrated to get an optimal representation of water levels, including the largest tidal constituent M2. In 3D DCSM-FM, the mean water levels imposed at the open boundaries have been adjusted with a uniform value to obtain an optimal M2 phase error along the Dutch coast. Nonetheless, with a similar phase error, 3D DCSM-FM produces a better representation of the M2 amplitude. The exact reason for this is unclear but might be related to a different representation of the Mean Dynamic Topography or different numerical settings for the Coriolis term.

Table 3.6 Overview of the 10 tidal components that have the largest contribution (in terms of vector difference) to the tidal error for the subset of 16 'coastal' stations (see Table 3.3)

Coastal stations							
2D DCSM-FM 0.5nm				**3D DCSM-FM**			
Comp.	Ampl. error (cm)	Phase error (º)	VD (cm)	Comp.	Ampl. error (cm)	Phase error (º)	VD (cm)
M2	-1.5	0.0	3.3	SA	1.3	-15.5	3.0
H1	-1.6	-60.2	2.0	M2	0.6	-0.1	2.9
SA	-1.3	-7.1	1.7	M4	0.6	2.3	1.7
M4	-0.3	3.6	1.7	H1	-1.0	-48.1	1.7
S2	-0.5	-0.2	1.6	S2	0.2	-0.3	1.5
2MS6	0.0	-1.5	1.3	SSA	-1.4	1.1	1.4
M6	0.0	-1.9	1.3	H2	0.7	49.3	1.2
SSA	-1.0	11.8	1.2	M6	-0.2	1.2	1.1
K1	0.5	-6.7	1.1	2MS6	0.0	1.6	1.1
N2	-0.6	1.2	1.0	S1	-0.1	-92.1	1.1

3.3.4 Skew surge (high waters)

3.3.4.1 3D DCSM-FM

The error statistics for three skew surge categories, at the Dutch coastal stations, can be found in Table 3.7. The numbers for all shelf-wide stations can be found in Appendix A.1.2. A spatial overview of the RMSE of the high-water skew surge (<99.0%, i.e., calm conditions) in the Dutch coastal stations is presented in Figure 3.9. This shows a skew surge error of about 4-5 cm in North Sea waters. In the eastern Wadden Sea and Dutch estuaries, the error increases to about 6 cm. The high-water skew surge is less sensitive to the quality with which the tide is represented (compared to the surge), which yields a more uniform model quality.

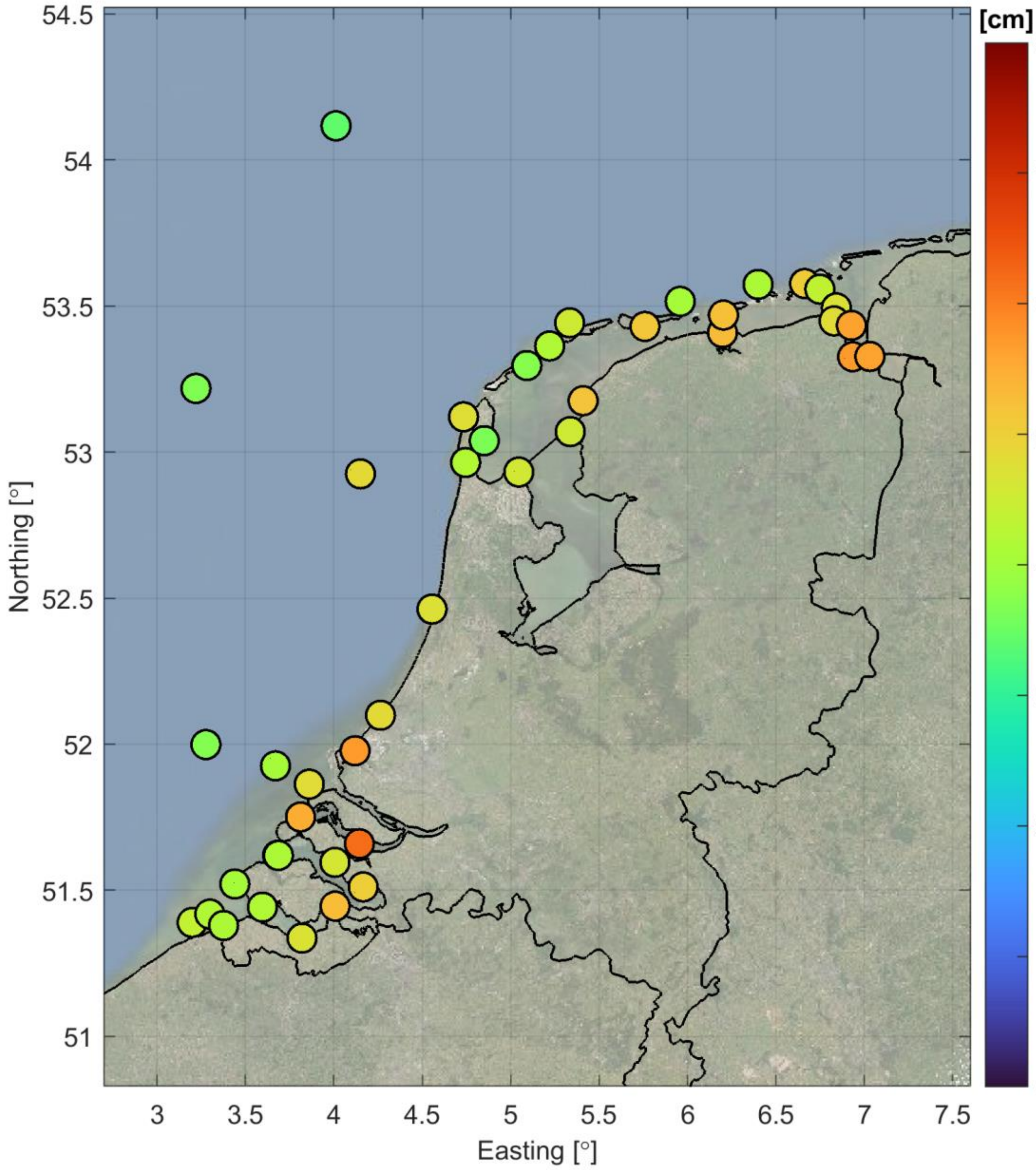

Figure 3.9 Spatial overview of the RMSE (cm) of the skew surge height for high waters (<99.0% skew surges)

In Figure 3.10, the bias and RMSE of the most extreme (>99.8%) skew surge events are presented. This shows an excellent quality in southern waters, with RMSE values mostly between 5-15 cm. One notable exception in that region is Brouwershavense Gat, which exhibits a bias of -19.1 cm and consequently has an RMSE of 20.7 cm. This is presumably caused by the presence of seiches during storms, which are not represented in the model.

Stations in the north, especially inside the Wadden Sea show larger skew surge errors. This is mostly due to a large systematic underestimation of the skew surge during storms. The bias is generally largest in the eastern part of the Wadden Sea and increases from north to south. In the Ems-Dollard the bias can reach 40-60 cm.

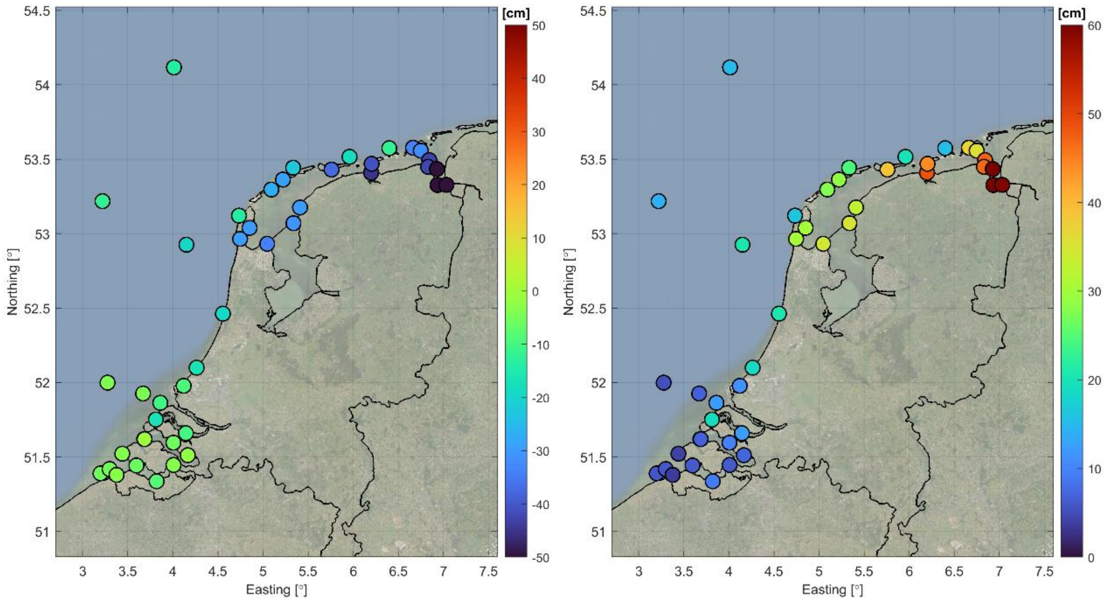

Figure 3.10 Spatial overview of the bias in cm (left panel) and RMSE in cm (right panel) of the skew surge height for high waters (>99.8% skew surges)

Table 3.7 Overview of the model skill to represent skew surge heights (high waters), for three different event classes, in terms of bias (cm) and the RMSE (cm) for Dutch coastal stations

Station	**<99.0% skew surges**		**99.0% - 99.8% skew surges**		**>99.8% skew surges**		
	bias (cm)	RMSE (cm)	bias (cm)	RMSE (cm)	bias (cm)	std (cm)	RMSE (cm)
Bol_Van_Heist	-1.0	4.3	-4.2	8.3	-4.6	4.2	6.2
Scheur_Wielingen_.	-0.4	4.2	-4.9	8.6	-5.7	2.3	6.2
CADZD	-0.2	4.3	-4.4	8.1	-3.6	6.9	7.8
WESTKPLE	0.3	4.0	-2.0	5.5	-4.9	2.8	5.7
EURPFM	-0.3	3.7	-3.6	7.3	-3.9	3.0	4.9
VLISSGN	0.3	4.2	-4.0	8.0	-4.7	3.4	5.7
ROOMPBTN	-0.5	4.2	-6.1	9.2	-11.6	2.4	11.8
LICHTELGRE	-0.4	4.0	-3.2	6.1	-4.7	5.4	7.2
BROUWHVSGT08	-1.4	5.3	-10.7	13.8	-19.1	7.8	20.7
TERNZN	0.7	4.6	-6.3	10.8	-3.7	5.6	6.7
HARVT10	-0.6	4.9	-6.5	10.9	-8.9	6.1	10.8
HANSWT	1.0	5.1	-1.7	9.7	-0.6	6.1	6.1
ROOMPBNN	-1.0	4.0	-1.1	5.6	-6.0	4.4	7.4
HOEKVHLD	-3.3	5.8	-7.7	10.5	-12.1	8.4	14.7
STAVNSE	0.4	4.7	-0.9	6.5	-7.3	9.0	11.5
BERGSDSWT	0.7	4.9	2.5	7.1	-6.9	8.8	11.2
KRAMMSZWT	-0.5	6.7	-7.2	11.6	-8.4	11.3	14.1
SCHEVNGN	-1.3	4.8	-7.7	10.3	-14.4	7.5	16.2
IJMDBTHVN	-0.9	4.8	-8.0	10.4	-16.8	7.0	18.2
Q1	-0.8	5.0	-6.9	11.0	-13.6	11.2	17.6
DENHDR	-0.7	4.1	-10.5	11.3	-22.2	11.3	24.9
TEXNZE	-1.4	4.7	-11.3	14.6	-14.7	7.1	16.3
K13APFM	-0.3	3.6	-4.9	8.4	-6.9	6.3	9.3

F16	-0.5	3.4	-5.6	7.7	-9.9	6.3	11.7
OUDSD	-0.2	3.7	-9.4	10.4	-22.8	10.2	25.0
DENOVBTN	-0.8	4.7	-12.6	13.9	-25.7	12.5	28.6
TERSLNZE	-1.2	4.6	-10.0	13.4	-17.5	10.6	20.4
VLIELHVN	-0.1	3.8	-10.0	11.5	-24.3	7.4	25.4
WESTTSLG	-0.2	4.1	-9.4	11.6	-25.6	7.0	26.6
KORNWDZBTN	-0.5	4.6	-11.9	14.9	-27.0	14.3	30.6
WIERMGDN	-0.5	4.2	-5.2	10.0	-15.6	7.2	17.2
HUIBGT	-0.6	4.5	-3.5	8.1	-10.4	8.3	13.3
HARLGN	0.0	5.1	-10.3	14.2	-26.0	11.8	28.6
NES	0.3	5.1	-15.4	17.9	-32.7	10.5	34.3
LAUWOG	0.5	5.6	-16.1	19.0	-39.6	16.6	42.9
SCHIERMNOG	0.5	5.2	-15.8	18.8	-36.3	14.2	39.0
BORKUM_Sudstran.	-0.2	4.9	-13.3	16.1	-34.4	12.8	36.7
BorkumFischerbalje	0.0	4.3	-10.0	13.7	-30.6	13.7	33.5
EMSHORN	0.0	4.7	-17.1	20.1	-43.4	16.7	46.5
EEMSHVN	-0.3	4.8	-17.0	19.9	-41.1	15.9	44.1
DUKEGAT	-0.4	5.3	-18.7	23.3	-59.8	21.9	63.6
DELFZL	-0.5	5.6	-17.8	22.1	-59.0	19.6	62.1
KNOCK	0.4	5.5	-15.6	20.1	-52.5	20.2	56.2
Average (total)	-0.4	4.6	-8.5	12.1	-19.5	9.4	22.0
Average (offshore)	-0.5	4.0	-4.8	8.1	-7.8	6.4	10.2
Average (coast)	-0.9	4.6	-6.8	10.2	-12.1	6.7	14.0
Average (SWD)	0.2	4.9	-2.7	8.5	-5.4	6.9	9.0
Average (WS)	-0.1	4.8	-13.8	16.7	-36.3	14.1	39.0

3.3.4.2 Comparison against 2D DCSM-FM 0.5nm

In Table 3.8 the station-averaged statistics, based on the stations in Dutch coastal waters, for 2D DCSM-FM 0.5nm (with HiRLAM and ERA5 meteorological forcing) and 3D DCSM-FM are given. This shows that the results for normal conditions (<99.0 % skew surges) improve (RMSE from 5.4 cm to 5.1 cm) when applying meteorological data from ERA5 instead of HiRLAM. However, in storm and extreme storm conditions, this change in source of meteorological forcing leads to an increase of the station-averaged RMSE (all stations) of about 1 cm. This increase is due a deterioration in the Wadden Sea stations. In the other regions, the quality under extreme storm conditions improves when using ERA5 meteorological forcing.

The model skill to represent the skew surge heights during normal conditions, shows that the three-dimensional model (3D DCSM-FM) has an average RMSE-value that is 0.5 cm less than the depth-averaged model (2D DCSM-FM 0.5nm), which is a 10% improvement. During storm conditions (99.0% - 99.8% skew surges), the quality of both models is similar. The statistics for the extreme storm conditions are slightly worse but note that these values are based on only a few events (>99.8 % skew surges).

Table 3.8 Comparison of the station-averaged model skill to represent skew surge heights (high waters), for three different event classes, in terms of bias (cm) and the RMSE (cm) for Dutch coastal stations.

	<99.0% skew surges		99.0% - 99.8% skew surges		>99.8% skew surges		
Total	bias (cm)	RMSE (cm)	bias (cm)	RMSE (cm)	bias (cm)	std (cm)	RMSE (cm)
2D DCSM-FM (HiRLAM)	-0.1	5.4	-0.8	9.6	-8.0	9.7	14.8
2D DCSM-FM (ERA5)	-0.1	5.1	-6.7	10.7	-12.8	7.7	15.7
3D DCSM-FM	-0.2	4.6	-7.0	10.6	-14.1	7.9	16.8
Offshore							
2D DCSM-FM (HiRLAM)	-0.3	4.6	-0.4	7.4	-7.7	9.8	13.0
2D DCSM-FM (ERA5)	-0.3	4.3	-4.8	8.3	-6.4	5.3	8.4
3D DCSM-FM	-0.5	4.0	-4.8	8.1	-7.8	6.4	10.2
Coast							
2D DCSM-FM (HiRLAM)	-1.0	5.6	-1.2	10.7	-9.3	10.1	14.3
2D DCSM-FM (ERA5)	-1.0	5.2	-7.0	10.7	-11.3	6.5	13.2
3D DCSM-FM	-0.9	4.6	-6.8	10.2	-12.1	6.7	14.0
South-western Delta							
2D DCSM-FM (HiRLAM)	0.1	6.1	6.2	11.8	2.5	9.2	9.9
2D DCSM-FM (ERA5)	0.1	5.4	-2.7	8.9	-4.7	7.3	9.3
3D DCSM-FM	0.2	4.9	-2.7	8.5	-5.4	6.9	9.0
Wadden Sea							
2D DCSM-FM (HiRLAM)	-0.1	5.7	-2.5	11.4	-26.4	14.9	30.7
2D DCSM-FM (ERA5)	-0.1	5.3	-11.8	15.5	-32.9	12.8	35.4
3D DCSM-FM	-0.1	4.8	-13.8	16.7	-36.3	14.1	39.0

4 Salinity, temperature and residual current validation

4.1 Water temperature

4.1.1 Sea surface temperature

In this section, the computed sea surface temperature is compared to in-situ measurements for the seven-year period 2006-2012 at the locations shown in Figure 4.1.

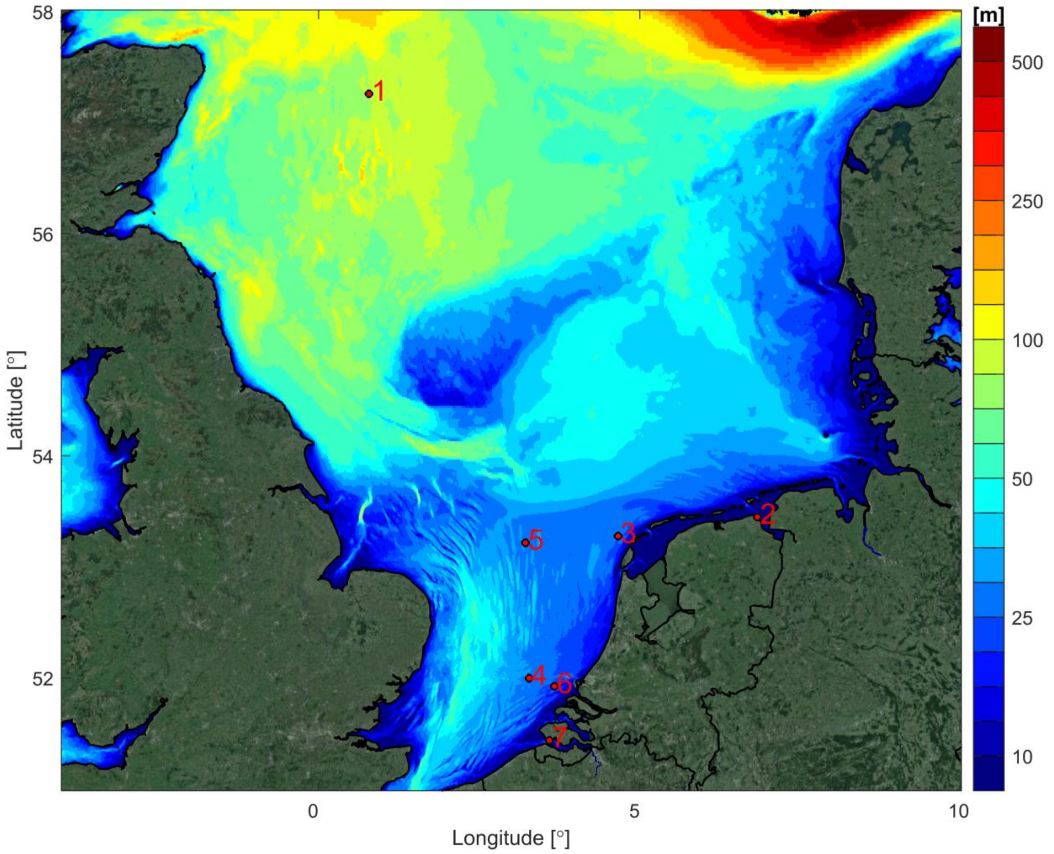

Figure 4.1 Locations of sea surface temperature measurements, with on the background the model depth (m +MSL). The numbers refer to the station numbers in Table 4.1.

In Figure 4.2 to Figure 4.4, a selection of three computed sea surface temperature time series are plotted together with the measured values. These results show that the inter-annual variability is well represented. Also, spatially, the model is capable of capturing the variation in seasonal temperature amplitude with less variability offshore (Anasuria and Platform K13a) and more in coastal and estuarine location (e.g. Vlissingen). The quality of the temperature representation is also shown quantitatively in Table 4.1. These results show a systematic underestimation of sea surface temperature by on average 0.34 °C and an average RMSE of 0.53 °C.

Table 4.1 Overview of the quality of the sea surface temperature representation in 3D DCSM-FM, in terms of bias, standard deviation (std) and Root-Mean-Square Error (RMSE).

#	Station name	bias (°C)	std (°C)	RMSE (°C)
1	Anasuria	-0.53	0.49	0.73
3	Eierlandse Gat	-0.44	0.36	0.57
6	Europlatform	-0.20	0.39	0.44
5	Platform K13a	-0.42	0.43	0.60
4	Lichteiland Goeree	-0.19	0.36	0.41
7	Vlissingen	-0.40	0.25	0.47
2	Eemshaven	-0.23	0.42	0.48
	Average	-0.34	0.39	0.53

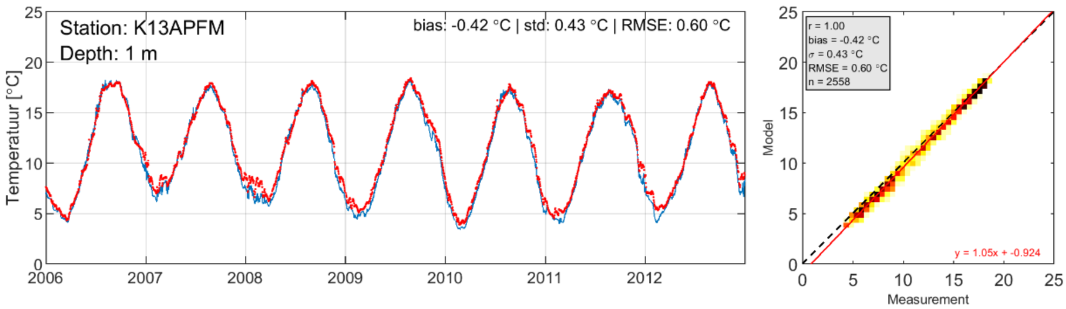

Figure 4.2 Time series of computed sea surface temperature (blue lines; 3D DCSM-FM) for station Platform K13a together with measured values (red dots).

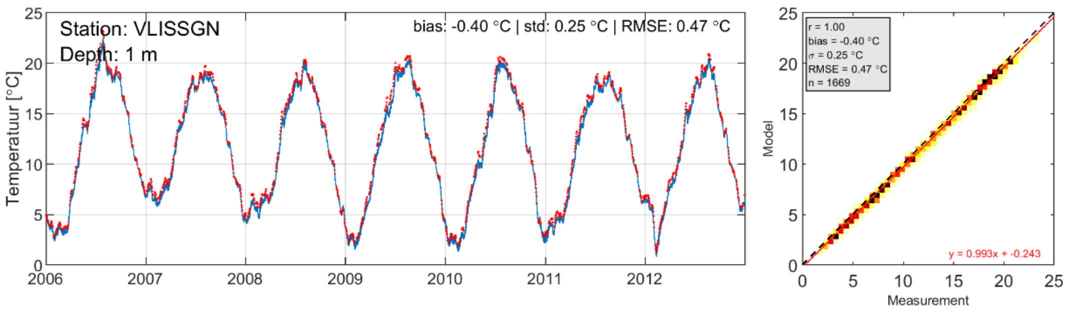

Figure 4.3 Time series of computed sea surface temperature (blue lines; 3D DCSM-FM) for station Vlissingen together with measured values (red dots).

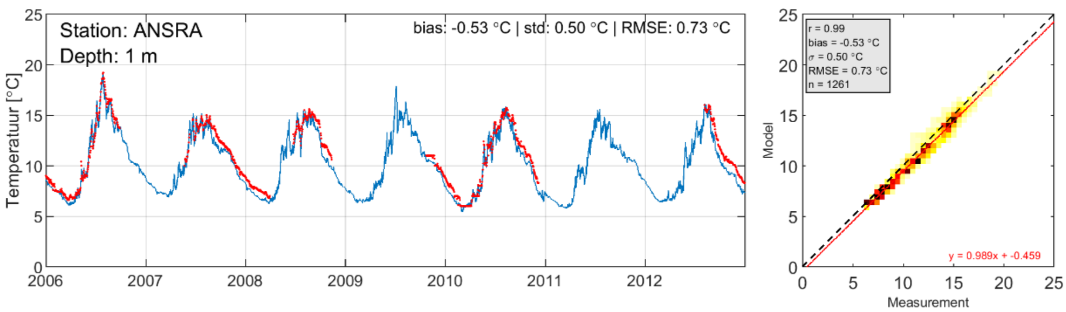

Figure 4.4 Time series of computed sea surface temperature (blue lines; 3D DCSM-FM) for station Anasuria together with measured values (red dots).

4.1.2 Temperature stratification in the central North Sea

Transport in the North Sea is affected by seasonal temperature stratification in the central North Sea. The relevance of this is illustrated with the fact that in the past, underprediction of the inter-annual variation of temperature stratification by ZUNO-DD was given as the main reason for explaining incorrect oxygen profiles in subsequent primary production simulations.

In Figure 4.5 the location of a station is indicated where both surface and bottom temperature are measured (at 1 m and 35 m below surface). In Figure 4.6 these are plotted as time series and compared with model results of 3D DCSM-FM. These results show that there is a good match with both surface and bottom temperature measurements (RMSE 0.55 °C and 0.70 °C, respectively). The bias at the surface is virtually the same as near the bed, which points to a correct representation of temperature stratification. This is also shown in Figure 4.7 where the modelled and measured vertical temperature differences are plotted together. This figure clearly shows that the average stratification is well represented, with a bias of just 0.12 °C. The maximum vertical temperature difference exhibits a strong inter-annual variation, with annual maxima varying between 6-12 °C. This variation is well captured by the model.

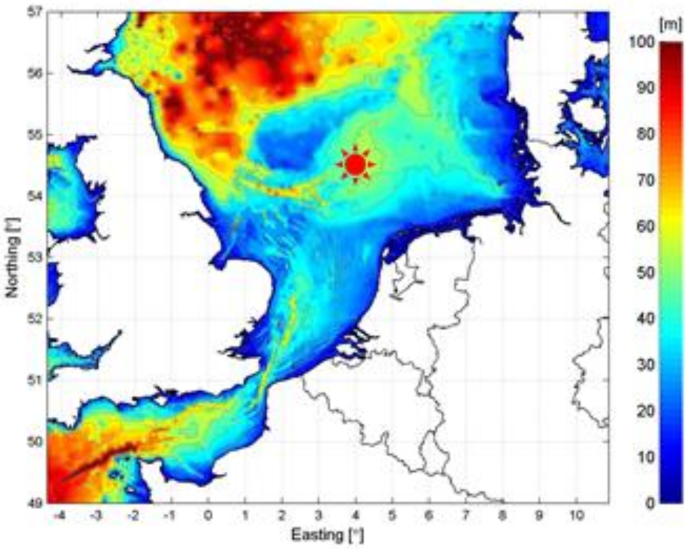

Figure 4.5 Location of station NL02, where water temperature is measured at 1m and 35 m below the surface.

Deltares

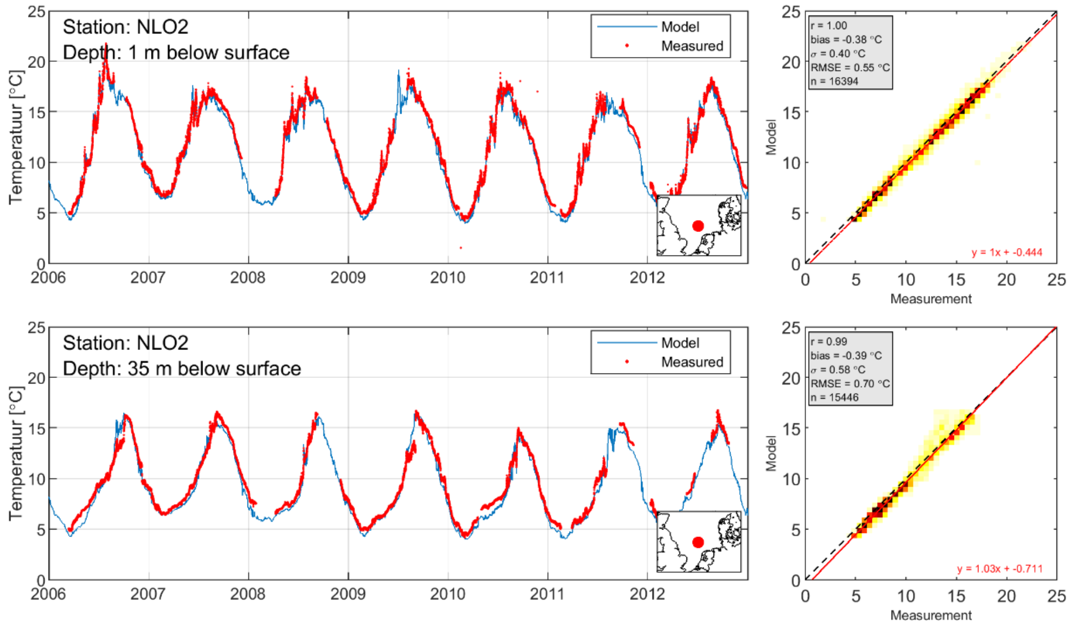

Figure 4.6 Time series of computed water temperature at 1 m (top) and 35 m (bottom) below surface (blue lines; 3D DCSM-FM) at station NL02 together with measured values (red dots).

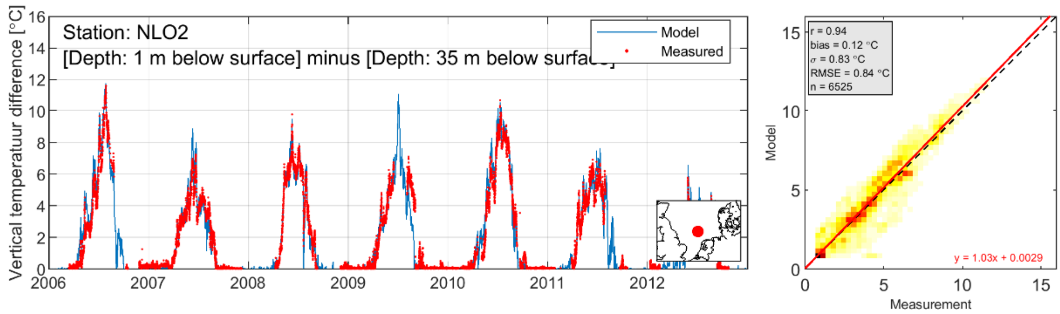

Figure 4.7 Time series of the vertical temperature difference (1m – 35 m below surface) at station NL02 (blue: 3D DCSM-FM; red: measurements).

4.2 Salinity

In this section computed sea surface salinity is compared to measurements along two transects for the ten-year period 2006-2015.

A quantitative assessment of the sea surface salinity representation is presented in Table 4.2 for the Noordwijk transect and in Table 4.3 for the Terschelling transect. The temporal variation in sea surface salinity is illustrated in time series plots of two locations (near the coast and offshore) for the Noordwijk transect (Figure 4.8 and Figure 4.9) and the Terschelling transect (Figure 4.10 and Figure 4.11).

These results show that, averaged over the locations in the transect, the model systematically underestimates the sea surface salinity with approximately 0.3 psu. The RMSE of sea surface salinity in the monitoring location closest to the coast is for both transects 1.4 psu. Further offshore, lower RMSE values are found, which coincides with having variability in (measured and modelled) sea surface salinity.

Table 4.2 Overview of the quality of the sea surface salinity representation in 3D DCSM-FM at the Noordwijk transect, in terms of bias, standard deviation (std) and Root-Mean-Square Error RMSE.

Station	bias (psu)	std (psu)	RMSE (psu)
Noordwijk 2 km	0.3	1.3	1.4
Noordwijk 10 km	-0.4	1.3	1.3
Noordwijk 20 km	-0.5	1.2	1.3
Noordwijk 70 km	-0.7	0.4	0.8
Average	-0.3	1.0	1.2

Table 4.3 Overview of the quality of the sea surface salinity representation in 3D DCSM-FM at the Terschelling transect, in terms of bias, standard deviation (std) and Root-Mean-Square Error RMSE.

Station	bias (psu)	std (psu)	RMSE (psu)
Terschelling 4 km	-0.7	1.2	1.4
Terschelling 10 km	-0.5	0.7	0.9
Terschelling 50 km	-0.5	0.4	0.7
Terschelling 100 km	-0.2	0.3	0.3
Terschelling 135 km	-0.1	0.4	0.4
Terschelling 175 km	-0.1	0.2	0.3
Terschelling 235 km	-0.1	0.2	0.3
Average	-0.3	0.5	0.6

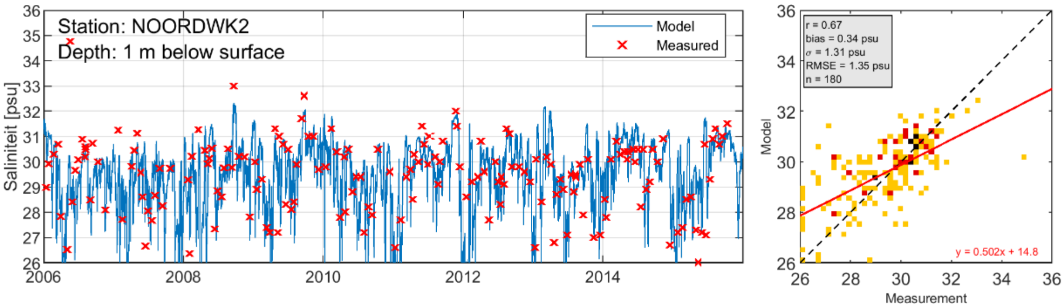

Figure 4.8 Time series of computed sea surface salinity (blue lines; 3D DCSM-FM) for station Noordwijk 2 km together with measured values (red dots).

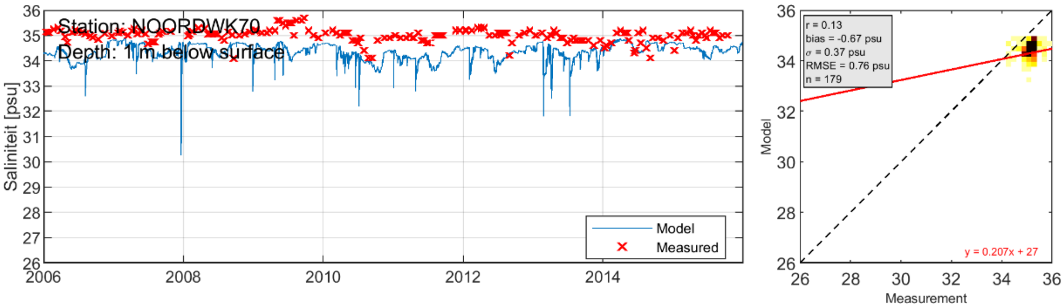

Figure 4.9 Time series of computed sea surface salinity (blue lines; 3D DCSM-FM) for station Noordwijk 70 km together with measured values (red dots).

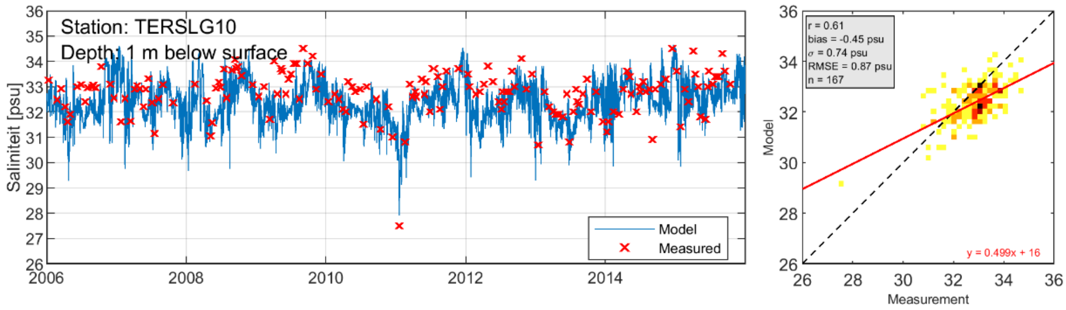

Figure 4.10 Time series of computed sea surface salinity (blue lines; 3D DCSM-FM) for station station Terschelling 10 km together with measured values (red dots).

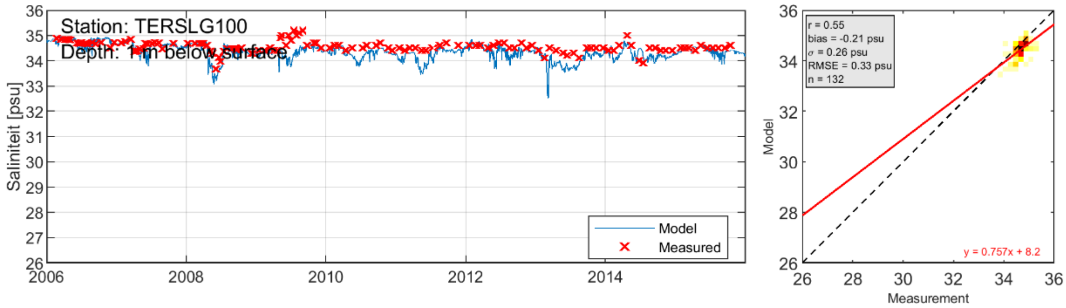

Figure 4.11 Time series of computed sea surface salinity (blue lines; 3D DCSM-FM) for station Terschelling 100 km together with measured values (red dots).

4.3 Residual transport through the English Channel

In the previous generation 3D ZUNO-DD model, tilting of the southern boundary was needed to achieve a correct representation of residual transport through the English Channel, which is estimated to be in the order of 100 x 10^3 m^3/s. Without tilting, the residual transport was considered too low. 3D DCSM-FM has a much larger model domain and thus there is no open boundary in the English Channel, which makes tilting impractical. Also, with a correct representation of the relevant physics in the model domain, this should not be required to get accurate results.

The residual transport through the English Channel is determined for the 10-year period 2006-2015, both for 2D DCSM-FM 0.5nm and 3D DCSM-FM. The results in Figure 4.12 show considerable inter-annual variation in residual transport, ranging from 43 x 10^3 m^3/s in 2010 to 153 x 10^3 m^3/s in 2014. Furthermore, with a long-term mean transport of 98 x 10^3 m^3/s, there is no need to artificially adjust the open boundaries. Comparison with the 2D results shows that the residual transport is mostly caused by barotropic phenomena. Adding salinity and temperature in the 3D configuration adds a further 15%.

Deltares

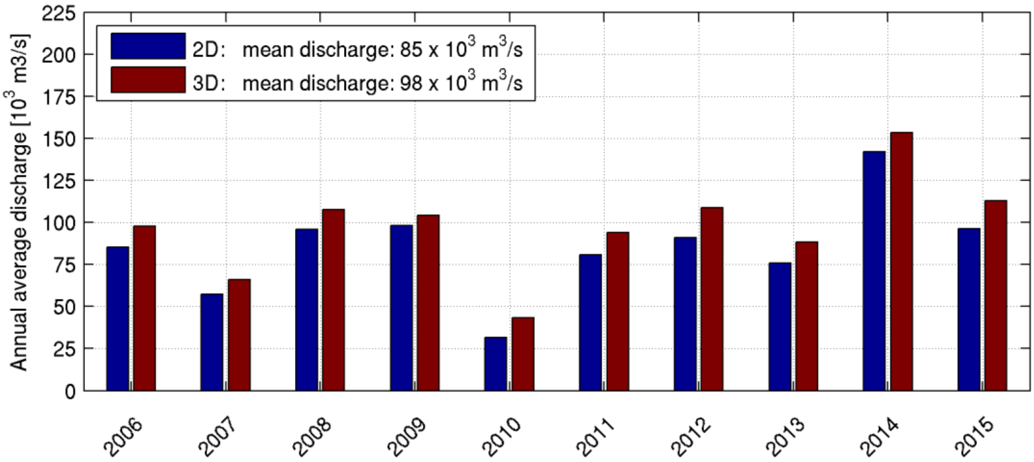

Figure 4.12 Annual average discharge through the English Channel computed with 3D DCSM-FM.

5 Conclusions and recommendations

5.1 Conclusions

In the past years, Deltares has worked on the development of a three-dimensional (3D) hydrodynamic model of the Northwest European Shelf: the 3D Dutch Continental Shelf Model in Flexible Mesh (3D DCSM-FM). Specifically, this model covers the North Sea and adjacent shallow seas and estuaries in the Netherlands, such as the Wadden Sea, the Ems-Dollard estuary, the Western Scheldt and the Eastern Scheldt. Rijkswaterstaat (Dutch Ministry of Infrastructure and Water Management) has requested Deltares to further develop and release this model as a sixth-generation model. This report describes the model setup and validation. With respect to the validation, the following can be concluded.

5.1.1 Water levels

3D DCSM-FM, forced with ERA5 meteorology, was validated against a set of shelf-wide stations (92 in total) for the period 2013-2017 and compared against the two-dimensional model DCSM-FM 0.5nm. An analysis of total water levels as well as the contribution of tide and surge showed that:

- Averaged over all shelf-wide stations an average RMSE for the tide of 9.1 cm, for the surge of 5.2 cm and for the total water level of 10.7 cm was found.
- Generally, the total water level RMSE is 6-8 cm in Dutch North Sea waters. In these stations, the tide and surge RMSE is generally 4-6 cm. The quality deteriorates inside the Dutch estuaries and Wadden Sea, where the model resolution is low compared to the variability in geometry and bathymetry.
- A comparison of 3D DCSM-FM against 2D DCSM-FM 0.5nm shows that the quality of the representation of the tide is, averaged over all Dutch coastal stations, very similar (5.0 cm vs. 5.1 cm). The surge RMSE decreases from 5.3 cm to 4.7 cm, which is a 10% reduction. With respect to total water levels, the 3D model results appear to be slightly better than the 2D model results, with the average RMSE decreasing from 7.3 cm to 6.9 cm.
- In Dutch waters, the amplitude and phase error of the M2 tidal constituent are generally less than 3 cm and 2°, respectively, in stations not hampered by a poor model resolution. Surprisingly, the contribution of M2 to the total tidal error in 3D DCSM-FM is less than in 2D DCSM-FM 0.5nm.
- Comparison against the previous generation 3D ZUNO-DD model of the southern North Sea shows that the total water levels along the Dutch coast, calculated by 3D DCSM-FM, are significantly better. The RMSE reduces by almost 75%, from 25.6 cm to 7.0 cm). This result is due to substantial improvements in both tide and surge.

The model is also assessed with respect to its capacity to represent the high water skew surge, i.e., the difference between a total high water and the associated astronomical high water, ignoring small differences in timing. This is done for three categories of events, subdivided based on the height of the measured skew surge. With respect to the skew surge the following can be concluded:

- The RMSE of the high-water skew surge (<99.0%, i.e., calm conditions) in the Dutch coastal stations is around 4-5 cm in North Sea waters. In the eastern Wadden Sea and Dutch estuaries, the error increases to about 6 cm.
- The most extreme (>99.8%) skew surge events shows an excellent quality in southern waters, with RMSE values mostly between 5-15 cm. Errors are much larger inside the (eastern) Wadden Sea, mostly due to a large systematic underestimation of the skew

surge during storms. In the Ems-Dollard the bias can reach 40-60 cm during these events.
- The model skill to represent the skew surge heights during normal conditions, shows that the three-dimensional model (3D DCSM-FM) has an average RMSE-value that is 0.5 cm less than the depth-averaged model (2D DCSM-FM 0.5nm), which is a 10% improvement. During storm conditions (99.0% - 99.8% skew surges), the quality of both models is similar. The statistics for the most extreme storm conditions are slightly worse in 3D DCSM-FM.

5.1.2 Sea surface temperature

- The sea surface temperature is well represented. This holds specifically for the inter-annual variability as well as the spatial variation of the seasonal amplitude.
- The average bias, standard deviation and RMSE in the stations assessed are 0.2-0.5 °C, 0.3-0.5 °C and 0.4-0.7 °C, respectively.
- The temperature in both the surface and bottom layer at station NL02 in the central North Sea matches well with measured values (RMSE 0.62 °C). Furthermore, the seasonal temperature stratification at this location, including its inter-annual variability, is well represented by the model (bias: 0.15 °C; RMSE: 0.79 °C).

5.1.3 Surface salinity

- The RMSE at the Noordwijk and Terschelling transect is on average 1.2 psu and 0.6, respectively. The sea surface salinity at these transects is systematically underestimated by on average 0.3 psu.

5.1.4 Residual transport through the English Channel

- In the previous generation 3D ZUNO-DD model, the open boundaries were artificially adjusted to achieve a realistic residual transport through the English Channel (which is estimated to be in the order of 100 x 10^3 m^3/s). 3D DCSM-FM, which has a much larger model domain, comes close to this value (98 x 10^3 m^3/s), without applying an artificial tilt.
- There is considerable inter-annual variation is residual transport, ranging from 43 x 10^3 m^3/s to 153 x 10^3 m^3/s.
- Comparison with the 2D results shows that the residual transport is mostly caused by barotropic phenomena. Adding salinity and temperature in the 3D configuration adds a further 15%.

5.2 Recommendations

5.2.1 Additional model validation

It is recommended to further validate the model against the recently prepared datasets of measured sea surface heights (2006-2013), including the low-frequency variability therein, and salinity- and temperature observations (Laan et al., 2020). These data are retrieved from several Dutch and international institutes/data sources. Furthermore, expanding the validation to the deeper, oceanic waters of the model should be considered.

5.2.2 Vertical layer distribution

Currently the model uses 20 equidistant sigma-layers to represent the vertical dimension. While this works well in the relatively shallow waters of the (southern) North Sea, this seems insufficient for representing relevant processes in the deep, oceanic waters of the model. Recent experiments have shown that the sea surface temperature in these areas can be improved by using a different vertical layer distribution (with a z-sigma layer approach). The improvement in temperature (stratification) there should be beneficial for the representation of the (semi-)annual water level variation in the model, the residual transport and the ability to represent the Mean Dynamic Topography (MDT, mean water level relative to a well-defined vertical reference plane).

5.2.3 Bathymetry

Outside Dutch coastal waters, the model bathymetry is based on the EMODnet October 2016 version. In the meantime, the more recent September 2018 version has become available and a 2020 version will become available at the end of 2020. Since significant bathymetry errors are known to exist in the October 2016 EMODnet bathymetry dataset, it is recommended to update the model bathymetry with the most recent version.

5.2.4 Boundary conditions

The tidal boundary conditions are based on the FES2012 global tide model. It is recommended to upgrade this to the most recently available version FES2014.

5.2.5 Meteorological forcing

The present validation was performed using ECMWF ERA5 meteorological forcing. Operationally, for 2D models Harmonie meteorological forcing is currently used, in addition to ECMWF IFS forcing. It is therefore recommended to further validate 3D DCSM-FM using Harmonie and ECMWF IFS meteorological forcing. Care should be taken with the way the wind forcing is applied. Currently, the use of stress (which is used to force the 2D fifth-generation models with Harmonie) prevents the application of the Relative Wind Effect, which has been shown to enhance the quality with which the surge is represented. Furthermore, besides the exchange of momentum, the exchange of mass (through evaporation and precipitation) as well as heat (through long wave and short-wave radiation and turbulent sensible and latent heat fluxes) is also considered in this 3D model. This has implications for the parameters that should be made available for operational use.

5.2.6 Mean Dynamic Topography

The water levels computed with 3D DCSM-FM (or any other hydrodynamic model) refer to an equipotential surface of the Earth's gravity field. Gradients in baroclinic pressure (i.e. due to density differences) affect the movement of water and can, consequently, affect the long-term mean water level (or Mean Dynamic Topography). While this these processes cannot explicitly be considered in a 2D model, this 3D model, including salinity and temperature as state parameters, is in principle capable to represent these phenomena, and therefore also the Mean Dynamic Topography. It is therefore recommended to validate this model with respect to its capability to directly compute water levels relative to a well-defined reference plane, such as NAP. If this is possible with sufficient accuracy, a post-processing correction such as currently applied operationally (the so-called bias-correction) would no longer be required.

6 Literature

Charnock, H. (1955). *Wind stress on a water surface*. Quarterly Journal of the Royal Meteorological Society, 81(350), 639-640.

EMODnet Bathymetry Consortium (2016). *EMODnet Digital Bathymetry (DTM).* http://doi.org/10.12770/c7b53704-999d-4721-b1a3-04ec60c87238.

Minns, A.W., Spruyt, A., Kerkhoven, D. (2019). *Specificaties zesde-generatie modellen met D-HYDRO; Generieke technische en functionele specificaties.* Deltares, report 11203714-013-ZWS-0001_v2.5.

Pawlowicz, R., Beardsley, B., Lentz, S. (2002). *Classical tidal harmonic analysis including error estimates in MATLAB using T_TIDE*. Computers and Geosciences 28 (2002), 929-937.

Zijl, F. (2016a). *Representation of the 18.6-year nodal cycle in DCSMv6*. Deltares, memo 1230072-003-ZKS-0007.

Zijl, F. (2016b). *The impact of relative wind effect on water levels*. Deltares, memo 1230072-003-ZKS-0008.

Zijl, F., Verlaan, M., Gerritsen, H., (2013). *Improved water-level forecasting for the Northwest European Shelf and North Sea through direct modelling of tide, surge and non-linear interaction*. Ocean Dyn. 63 (7).

Zijl, F., Groenenboom, J. (2019). *Development of a sixth-generation model for the NW European Shelf (DCSM-FM 0.5nm).* Deltares, report 11203715-004-ZKS-0003.

Zijl, F., Groenenboom, J., Laan, S.C.L. (2020). *Development of a sixth-generation model for the NW European Shelf (DCSM-FM 100m).* Deltares, report 11205259-004-ZKS-0001.

A Model validation

A.1 Shelf-wide results

A.1.1 Tide, surge and total water level

Table A.1 Statistics (RMSE-values in cm) of tide, surge and total water level of 2D DCSM-FM 0.5nm (with meteorological forcing HiRLAM and ERA5) and 3D DCSM-FM for all shelf-wide tide gauge stations.

Station	RMSE tide (cm)			RMSE surge (cm)			RMSE water level (cm)		
	2D DCSM-FM 0.5nm (HiRLAM)	2D DCSM-FM 0.5nm (ERA5)	3D DCSM-FM 0.5nm	2D DCSM-FM 0.5nm (HiRLAM)	2D DCSM-FM 0.5nm (ERA5)	3D DCSM-FM 0.5nm	2D DCSM-FM 0.5nm (HiRLAM)	2D DCSM-FM 0.5nm (ERA5)	3D DCSM-FM 0.5nm
A2	5.2	5.2	5.1	5.1	5.0	4.7	7.3	7.2	6.9
ABDN	4.8	5.1	5.4	4.6	4.5	4.0	6.6	6.7	6.8
BANGR	12.2	12.2	11.1	4.6	4.4	3.9	13.1	13.1	11.7
BARMH	13.5	13.8	13.5	6.6	7.2	6.8	14.8	15.5	15.1
BERGSDSWT	11.0	11.3	13.2	6.2	6.0	5.6	12.6	12.8	14.3
BORKUM_Sudstrand	7.3	7.3	6.9	5.7	5.7	5.4	9.2	9.3	8.7
BOURNMH							6.3	6.3	6.6
BROUWHVSGT08	6.1	6.1	5.2	6.1	6.0	5.2	8.5	8.5	7.3
Bol_Van_Heist	5.5	5.5	5.6	5.2	5.1	4.4	7.5	7.5	7.2
BorkumFischerbalje	6.7	6.7	6.4	5.7	5.5	4.9	8.8	8.6	8.0
CADZD	5.8	5.7	4.6	5.7	5.6	4.7	8.1	8.0	6.6
CROMR	8.0	8.1	8.8	6.7	6.2	5.8	9.4	9.1	9.2
DELFZL	10.8	10.5	9.7	7.9	7.9	7.3	13.4	13.2	12.1
DENHDR	4.2	4.4	4.5	5.1	5.1	4.5	6.6	6.7	6.4
DENOVBTN	7.4	7.8	6.0	6.9	6.6	6.2	10.1	10.2	8.7
DEVPT	13.4	13.5	13.3	4.5	4.5	4.1	14.2	14.3	14.1
DOVR	8.9	8.9	10.6	4.4	4.3	4.2	9.7	9.7	11.1
DUKEGAT	8.0	7.8	7.3	7.0	6.8	6.3	10.1	9.9	9.2
EEMSHVN	7.2	7.0	6.1	6.2	6.1	5.5	9.5	9.2	8.2
EMSHORN	7.6	7.4	6.4	6.1	6.2	5.6	9.7	9.6	8.5
EURPFM	3.7	3.7	3.8	4.7	4.4	3.8	5.8	5.6	5.4
F16	3.0	3.3	3.4	4.1	3.9	3.4	5.0	5.2	4.8
F3PFM	3.6	3.7	3.0	4.5	4.3	3.7	5.5	5.5	4.7
FISHGD	6.8	6.7	6.1	4.4	4.3	4.3	7.7	7.7	7.2
HANSWT	18.9	19.2	19.3	7.1	7.3	6.5	20.2	20.5	20.4
HARLGN	8.7	8.8	7.0	6.8	6.5	6.3	11.0	10.9	9.4
HARVT10	4.3	4.4	4.5	5.4	5.0	4.8	6.9	6.7	6.6
HARWH	13.6	13.6	13.5	6.9	6.3	5.8	14.9	14.7	14.3
HEYSHM	28.7	29.0	30.5	7.8	7.5	7.3	29.6	29.7	31.1
HINKLPT	13.0	13.3	17.2	7.2	7.2	6.6	14.7	15.0	18.2
HOEKVHLD	4.4	4.7	5.5	5.8	5.4	4.9	7.3	7.1	7.3
HOLHD	6.8	7.0	7.0	4.3	4.2	3.4	8.1	8.1	7.7
HOLWD	31.0	31.2	29.9	14.6	14.8	14.5	34.3	34.5	33.2
HUIBGT	5.2	5.0	5.0	5.7	5.3	5.0	7.5	7.0	6.7

IJMDBTHVN	5.4	5.6	6.1	5.8	5.6	5.0	7.9	7.9	7.9
ILFCBE	10.0	10.0	7.5	4.9	4.9	4.4	11.0	11.0	8.7
IMMHM	16.2	16.2	15.5	8.7	8.2	7.2	18.5	18.4	17.1
K13APFM	4.3	4.5	4.9	4.4	4.2	3.8	6.1	6.1	6.2
KINLBVE	7.3	7.7	7.7	5.0	4.6	4.4	7.7	7.7	7.5
KNOCK	11.0	10.7	10.1	7.7	7.8	7.1	13.4	13.2	12.4
KORNWDZBTN	4.6	4.9	4.4	5.7	5.3	5.2	7.3	7.2	6.9
KRAMMSZWT	8.1	8.4	10.7	6.3	6.3	5.7	10.2	10.5	12.1
LAUWOG	14.2	14.1	13.4	7.5	7.6	7.6	16.0	16.1	15.4
LEITH	10.3	10.3	9.4	6.4	6.0	5.6	12.1	11.9	11.0
LERWK	4.3	4.5	3.7	3.7	3.6	3.5	5.6	5.7	5.2
LICHTELGRE	4.7	4.8	4.6	4.7	4.4	4.1	6.7	6.5	6.1
LIVPL	17.4	17.5	18.1	7.1	7.3	7.3	18.3	18.4	19.2
LLANDNO	7.6	7.7	8.5	5.5	5.4	4.8	9.4	9.4	9.6
LOWST	5.1	5.1	5.6	5.3	4.7	4.5	7.2	6.8	7.1
MILFHVN	7.1	7.0	5.6	4.9	4.7	4.2	8.1	8.0	6.8
MILLPT	18.5	18.5	16.7	6.2	5.8	5.2	19.4	19.3	17.4
MUMBS	9.3	9.4	8.3	5.2	5.3	4.6	12.7	12.8	10.8
MalinHead	9.5	9.6	8.8	6.2	6.0	5.2	11.3	11.3	10.1
NES	15.4	15.4	14.1	7.6	8.0	7.6	17.2	17.4	16.0
NEWHVN	11.2	11.3	12.2	4.2	4.0	3.5	12.0	11.9	12.7
NEWLN	4.4	4.5	5.3	3.8	3.8	3.2	5.7	5.8	6.0
NEWPT							29.0	29.8	28.4
NORTHCMRT	5.0	5.2	4.6	4.4	4.3	3.7	6.5	6.6	5.7
NORTHSS	8.6	8.7	8.7	5.0	4.7	4.3	9.9	9.8	9.6
OUDSD	4.6	4.8	5.0	4.7	4.6	4.1	6.6	6.6	6.5
Oostende	6.8	6.8	7.6	5.2	5.0	4.5	8.6	8.5	8.8
PORTERIN	5.9	6.1	6.4	4.1	4.1	3.5	7.2	7.3	7.3
PORTPTK	10.6	10.7	9.4	4.4	4.5	3.8	11.5	11.6	10.1
PORTRH	7.2	7.4	7.1	4.6	4.3	3.7	8.3	8.3	7.8
PORTSMH	18.6	18.6	19.7	5.1	5.0	4.9	19.1	19.1	20.1
PortTudy	8.9	9.0	8.8	4.8	4.7	4.0	9.8	9.9	9.4
Portbury	59.2	59.5	53.0	17.0	17.2	16.4	62.1	62.5	55.7
Q1	4.2	4.4	5.1	4.6	4.5	4.0	6.3	6.3	6.5
ROOMPBNN	4.4	4.5	5.9	4.9	4.8	4.2	6.6	6.6	7.2
ROOMPBTN	3.8	3.9	4.5	5.0	4.9	4.4	6.3	6.3	6.2
SCHEVNGN	4.5	4.7	5.1	5.6	5.3	4.7	7.1	7.0	6.9
SCHIERMNOG	24.2	24.4	23.6	9.9	10.1	9.8	26.1	26.3	25.6
SHEERNS							18.2	17.5	16.9
STAVNSE	5.5	5.7	7.9	5.4	5.4	4.9	7.7	7.9	9.3
STMARYS							5.0	5.0	5.5
STORNWY	8.3	8.4	8.3	5.0	4.7	4.2	8.8	8.8	8.6
Scheur_Wielingen_B.	5.7	5.6	5.1	5.4	5.2	4.6	7.7	7.5	6.8
TERNZN	6.7	7.0	7.1	6.2	6.3	5.5	9.1	9.4	9.0
TERSLNZE	4.4	4.4	4.2	5.6	5.4	4.8	7.1	6.9	6.3
TEXNZE	5.0	5.1	5.9	5.6	5.4	5.0	7.4	7.3	7.6
TOBMRY	7.0	7.1	7.1	4.5	4.2	3.7	8.3	8.2	8.0
ULLPL	7.7	8.0	8.0	5.4	5.0	4.6	10.4	10.4	9.8
VLIELHVN	3.8	4.1	4.6	5.0	5.0	4.5	6.3	6.4	6.5

VLISSGN	6.3	6.3	5.4	5.6	5.6	4.8	8.4	8.5	7.2
WESTKPLE	6.3	6.2	5.2	5.1	5.1	4.3	8.1	8.0	6.8
WESTTSLG	4.8	5.0	6.2	5.0	4.9	4.7	7.0	7.0	7.8
WEYMH	4.7	4.8	5.2	4.0	3.9	3.6	5.8	5.8	6.2
WHITBY	8.9	9.0	8.9	5.5	5.3	4.6	10.6	10.6	10.0
WICK	5.3	5.5	5.6	4.5	4.5	4.2	6.5	6.6	6.5
WIERMGDN	4.8	4.7	4.4	5.5	5.1	4.5	7.2	6.9	6.2
WORKTN	9.8	9.9	10.0	5.4	5.3	4.7	11.2	11.2	11.1
Westhinder	6.6	6.6	6.5	4.9	4.6	4.1	8.1	7.9	7.5

A.1.2 High waters

Table A.2 Overview of the 3D DCSM-FM model skill to represent skew surge heights (high waters), for three different event classes, in terms of bias (cm) and the RMSE (cm) for all shelf-wide tide gauge stations.

Station	<99.0% skew surges		99.0% - 99.8% skew surges		>99.8% skew surges		
	bias (cm)	RMSE (cm)	bias (cm)	RMSE (cm)	bias (cm)	std (cm)	RMSE (cm)
A2	-0.5	4.5	-3.6	8.7	-1.0	5.6	5.7
ABDN	-0.3	3.9	-5.0	6.2	-6.7	2.7	7.3
BANGR	0.4	3.6	-6.7	9.0	-9.4	3.9	10.2
BARMH	-0.9	5.5	-16.3	19.3	-27.8	14.1	31.2
BERGSDSWT	0.7	4.9	2.5	7.1	-6.9	8.8	11.2
BORKUM_Sudstran.	-0.2	4.9	-13.3	16.1	-34.4	12.8	36.7
BROUWHVSGT08	-1.4	5.3	-10.7	13.8	-19.1	7.8	20.7
Bol_Van_Heist	-1.0	4.3	-4.2	8.3	-4.6	4.2	6.2
BorkumFischerbalje	0.0	4.3	-10.0	13.7	-30.6	13.7	33.5
CADZD	-0.2	4.3	-4.4	8.1	-3.6	6.9	7.8
CROMR	0.3	5.6	-1.1	5.3	-2.4	11.1	11.3
DELFZL	-0.5	5.6	-17.8	22.1	-59.0	19.6	62.1
DENHDR	-0.7	4.1	-10.5	11.3	-22.2	11.3	24.9
DENOVBTN	-0.8	4.7	-12.6	13.9	-25.7	12.5	28.6
DEVPT	0.8	3.6	-5.2	6.4	-7.7	5.3	9.4
DOVR	1.4	4.0	4.5	5.1	-1.6	0.4	1.6
DUKEGAT	-0.4	5.3	-18.7	23.3	-59.8	21.9	63.6
EEMSHVN	-0.3	4.8	-17.0	19.9	-41.1	15.9	44.1
EMSHORN	0.0	4.7	-17.1	20.1	-43.4	16.7	46.5
EURPFM	-0.3	3.7	-3.6	7.3	-3.9	3.0	4.9
F16	-0.5	3.4	-5.6	7.7	-9.9	6.3	11.7
F3PFM	-0.3	3.8	-7.7	8.7	-10.5	4.6	11.5
FISHGD	-1.9	4.2	-5.4	6.9	-13.3	2.8	13.6
HANSWT	1.0	5.1	-1.7	9.7	-0.6	6.1	6.1
HARLGN	0.0	5.1	-10.3	14.2	-26.0	11.8	28.6
HARVT10	-0.6	4.9	-6.5	10.9	-8.9	6.1	10.8
HARWH	0.7	6.7	-5.5	10.9	2.4	8.3	8.7
HEYSHM	1.3	7.0	-12.5	16.0	-14.6	1.7	14.7
HINKLPT	-0.1	5.4	-9.9	11.8	-15.9	12.9	20.5
HOEKVHLD	-3.3	5.8	-7.7	10.5	-12.1	8.4	14.7
HOLHD	-0.8	3.3	-6.6	8.4	-7.3	4.9	8.8
HOLWD	-0.1	7.5	-15.2	20.2	-37.6	15.8	40.8
HUIBGT	-0.6	4.5	-3.5	8.1	-10.4	8.3	13.3
IJMDBTHVN	-0.9	4.8	-8.0	10.4	-16.8	7.0	18.2
ILFCBE	-0.6	3.6	-5.8	7.3	-11.7	1.9	11.9
IMMHM	3.7	7.0	1.4	22.4	-13.3	3.5	13.7
K13APFM	-0.3	3.6	-4.9	8.4	-6.9	6.3	9.3
KINLBVE	-1.5	4.3	-5.9	8.7	-6.2	5.6	8.3
KNOCK	0.4	5.5	-15.6	20.1	-52.5	20.2	56.2
KORNWDZBTN	-0.5	4.6	-11.9	14.9	-27.0	14.3	30.6
KRAMMSZWT	-0.5	6.7	-7.2	11.6	-8.4	11.3	14.1

LAUWOG	0.5	5.6	-16.1	19.0	-39.6	16.6	42.9
LEITH	0.4	5.1	-5.8	10.9	-13.5	5.1	14.5
LERWK	-1.1	3.5	-2.7	4.9	-4.4	5.0	6.7
LICHTELGRE	-0.4	4.0	-3.2	6.1	-4.7	5.4	7.2
LIVPL	-1.7	5.8	-13.6	14.5	-23.3	13.8	27.0
LLANDNO	1.2	4.4	-3.4	6.5	-3.6	6.4	7.3
LOWST	-0.4	4.5	-2.5	8.1	-4.5	12.3	13.1
MILFHVN	-0.1	3.9	-4.3	8.0	-9.6	4.3	10.5
MILLPT	-0.2	4.9	-4.3	8.4	-9.2	5.7	10.8
MUMBS	0.5	3.6	-7.2	9.2	-15.4	1.5	15.5
MalinHead	0.2	5.4	-3.9	7.4	-4.9	5.9	7.6
NES	0.3	5.1	-15.4	17.9	-32.7	10.5	34.3
NEWHVN	0.0	3.4	-3.0	5.8	-3.4	10.2	10.7
NEWLN	-0.5	3.0	-3.9	5.2	-7.2	4.8	8.6
NORTHCMRT	0.0	3.6	-1.5	5.1	-2.4	6.8	7.2
NORTHSS	-0.3	4.1	-6.2	9.5	-8.6	7.8	11.6
OUDSD	-0.2	3.7	-9.4	10.4	-22.8	10.2	25.0
Oostende	-0.3	4.3	-4.9	8.6	-1.8	5.7	5.9
PORTERIN	-0.1	3.4	-6.0	7.7	-8.8	4.0	9.7
PORTPTK	-0.2	3.4	-8.0	9.2	-15.9	5.6	16.9
PORTRH	-0.5	3.9	-1.8	6.8	-1.6	5.1	5.3
PORTSMH	1.4	4.1	-3.9	7.1	-1.8	4.9	5.2
PortTudy	-0.7	3.8	-7.1	8.8	-6.9	6.8	9.7
Portbury	3.2	9.4	-11.7	16.2	-18.4	20.1	27.3
Q1	-0.8	5.0	-6.9	11.0	-13.6	11.2	17.6
ROOMPBNN	-1.0	4.0	-1.1	5.6	-6.0	4.4	7.4
ROOMPBTN	-0.5	4.2	-6.1	9.2	-11.6	2.4	11.8
SCHEVNGN	-1.3	4.8	-7.7	10.3	-14.4	7.5	16.2
SCHIERMNOG	0.5	5.2	-15.8	18.8	-36.3	14.2	39.0
STAVNSE	0.4	4.7	-0.9	6.5	-7.3	9.0	11.5
STORNWY	-1.0	4.2	-2.8	6.6	-8.9	2.7	9.3
Scheur_Wielingen_.	-0.4	4.2	-4.9	8.6	-5.7	2.3	6.2
TERNZN	0.7	4.6	-6.3	10.8	-3.7	5.6	6.7
TERSLNZE	-1.2	4.6	-10.0	13.4	-17.5	10.6	20.4
TEXNZE	-1.4	4.7	-11.3	14.6	-14.7	7.1	16.3
TOBMRY	0.1	3.5	-4.5	7.0	-6.9	6.1	9.2
ULLPL	-0.2	4.4	-8.8	11.1	-5.4	5.0	7.4
VLIELHVN	-0.1	3.8	-10.0	11.5	-24.3	7.4	25.4
VLISSGN	0.3	4.2	-4.0	8.0	-4.7	3.4	5.7
WESTKPLE	0.3	4.0	-2.0	5.5	-4.9	2.8	5.7
WESTTSLG	-0.2	4.1	-9.4	11.6	-25.6	7.0	26.6
WEYMH	-0.4	3.1	-5.7	8.0	-4.7	2.6	5.3
WHITBY	1.0	4.2	-6.4	9.0	-9.3	9.3	13.2
WICK	-0.4	4.2	-5.8	7.7	-10.4	5.3	11.7
WIERMGDN	-0.5	4.2	-5.2	10.0	-15.6	7.2	17.2
WORKTN	-0.2	4.4	-2.2	6.9	-3.2	6.2	6.9
Westhinder	-0.2	3.8	-1.6	5.7	-0.3	5.8	5.8

Deltares is an independent institute for applied research in the field of water and subsurface. Throughout the world, we work on smart solutions for people, environment and society.

Deltares

www.deltares.nl